

## ***Student Declaration Form for Submission with Major Projects***

This form must be completed by the student **and** included at the beginning of the Project Report.

Student's Name	GABRIEL PIERCE
Student's Number	22239009
Degree Programme	MENG Integrated Engineering (Accelerated)
Supervisor	Nadia kourra, Parakram Pyakurel
Project Title	Democratising Precision: An Open-Source, 3D-Printed Rotation Stage for Scientific Applications
Word Count	9416
Confidential?	No

*In submitting this Project report, I acknowledge that I understand the definition of, and penalties for, cheating, collusion and plagiarism set out in the assessment regulations. I also confirm that this work has not previously been submitted for assessment for an academic award, unless otherwise indicated.*

*Any AI, or LLM generated code, images or content used within your submission should be highlighted and accordingly referenced. Further, a footnote statement should follow the main body of work in the submission demonstrating your understanding of the issues of potential copyright infringement, by using AI or LLM tools. Where prompt engineering has been used, you should include a separate appendix containing all your prompts, to evidence that your own understanding and knowledge was used to provide the final content, rather than using AI generated knowledge*

(Electronic) Signature of student:G.Pierce

Date: 03/07/25



# **Democratising Precision: An Open-Source, 3D-Printed Rotation Stage for Scientific Applications**

GABRIEL PIERCE

being a Master's Engineering Project submitted in partial fulfilment  
of the requirements for the MEng Honours Degree in  
Integrated Engineering

# Contents

<b>Contents</b>	<b>1</b>
<b>List of Tables</b>	<b>3</b>
<b>List of Figures</b>	<b>4</b>
<b>Nomenclature</b>	<b>5</b>
<b>Abstract</b>	<b>6</b>
<b>Acknowledgements</b>	<b>7</b>
<b>1 Introduction</b>	<b>8</b>
1.1 Project Background and Objectives . . . . .	8
1.1.1 Objectives . . . . .	8
1.2 Problem Significance and Rationale . . . . .	9
1.3 Project Scope . . . . .	9
1.4 Project Constraints . . . . .	9
<b>2 Background Overview</b>	<b>10</b>
2.1 Introduction . . . . .	10
2.2 Computed Axial Lithography (CAL) . . . . .	10
2.2.1 Rotation Stage Requirements and Low-Cost Implementations . . . . .	10
2.2.2 Drive Mechanisms for Precision Rotation . . . . .	11
2.2.3 Bearings for Precision Rotation Stages . . . . .	11
2.3 Stepper Motor Control . . . . .	11
2.3.1 Closed-Loop Stepper Motor Control for Enhanced Precision . . . . .	12
2.3.2 Comparison of Control Strategies . . . . .	14
2.4 Backlash and Positional Error . . . . .	14
2.4.1 Impact, Measurement, and Mitigation . . . . .	15
2.5 Low-Cost and Open-Source Scientific Hardware . . . . .	15
2.5.1 Precedent in 3D-Printed Optical Mounts . . . . .	15
2.5.2 FOSH Case Studies and Design Philosophy . . . . .	15
2.5.3 Impact on Research Accessibility . . . . .	15
2.6 Informal Sources and Community Knowledge . . . . .	16
2.6.1 Cycloidal Drive Design . . . . .	16
<b>3 Methodology</b>	<b>17</b>
3.1 Introduction . . . . .	17
3.2 Methodological Framework . . . . .	17
3.3 Project Management and Risk Assessment . . . . .	18
3.4 The Stage-Gate Model . . . . .	19
3.5 The Iterative Design Process . . . . .	19
3.6 Application of the Stage-Gate Model . . . . .	20
3.7 Summary of Methodological Approach . . . . .	20

<b>4 System Design and Development</b>	<b>21</b>
4.1 Introduction . . . . .	21
4.2 Component and Material Selection . . . . .	21
4.3 Mechanical Design . . . . .	21
4.3.1 Cycloidal Drive Design and Parameters . . . . .	21
4.3.2 CAD Implementation and Prototyping . . . . .	22
4.4 Control Software Development . . . . .	23
4.4.1 System Architecture and Design . . . . .	23
4.4.2 Motion Command and Control Logic . . . . .	23
4.4.3 Position Feedback and Calibration . . . . .	24
4.4.4 Zero Point Synchronisation . . . . .	24
4.4.5 Safety and Usability . . . . .	24
<b>5 Testing and Results</b>	<b>25</b>
5.1 Precision Testing . . . . .	25
5.1.1 Repeatability and Backlash . . . . .	26
5.2 Output Torque . . . . .	26
5.2.1 Dynamic Load Performance . . . . .	26
5.3 Analysis of Results . . . . .	27
5.3.1 Precision Testing . . . . .	27
5.3.2 Defining an Acceptable Error Benchmark . . . . .	28
<b>6 Discussion</b>	<b>31</b>
6.1 Error in testing . . . . .	31
6.2 Interpolation and Control Limitations . . . . .	31
6.3 Comparison of Prototype Vs Thorlabs PRM1Z8 . . . . .	32
6.4 Price-to-Performance Analysis and Practical Significance . . . . .	32
6.5 Partially Printed Bearings . . . . .	32
6.6 Constraints of Additive Manufacturing . . . . .	33
6.7 Further Testing . . . . .	33
6.7.1 Observing Wear . . . . .	33
<b>7 Evaluation and Conclusion</b>	<b>34</b>
7.1 Project Evaluation . . . . .	34
7.1.1 Effectiveness of the Hybrid Methodological Framework . . . . .	34
7.1.2 Evaluation of Project Planning: The Gantt Chart . . . . .	34
7.1.3 Evaluation of Design Trade-offs . . . . .	34
7.2 Wider Context and Impact . . . . .	35
7.3 Lessons Learned . . . . .	35
7.4 Future Work and Recommended Improvements . . . . .	36
7.5 Conclusion . . . . .	36
<b>8 Appendices</b>	<b>40</b>
8.1 Project Files and Documentation . . . . .	40
8.2 CAD Equations . . . . .	41
8.3 Precision Data . . . . .	41
8.4 Gantt Chart . . . . .	56

# List of Tables

2.1	Key Components of a Typical CAL System. . . . .	10
2.2	Key Benefits of Closed-Loop Stepper Motor Control. . . . .	12
2.3	Comparison of Closed-Loop and Advanced Open-Loop Control Systems. . . . .	14
2.4	Common Positional Errors in Motion Systems. . . . .	14
3.1	Project Risk Assessment and Mitigation Strategies. . . . .	18
3.2	Project Risk Assessment After Mitigation. . . . .	18
4.1	Key Design Parameters of the Cycloidal Drive Prototype. . . . .	22
5.1	Summary of Dynamic Torque Test Results. . . . .	27
5.2	Theoretical Angular Resolution by Microstepping Setting for a $1.8^\circ$ Motor. . . . .	27
6.1	Performance Comparison of Prototype vs. Commercial Stage . . . . .	32

# List of Figures

2.1	A flow diagram of an open loop system vs a Closed loop system [26] . . . . .	12
3.1	An Example of a typical Stage gate process [42]. . . . .	19
3.2	An example of a typical Iterative Design Cycle [44]. . . . .	19
4.1	An illustration showing the components of a Cycloidal Drive [46]. . . . .	21
4.2	Cycloidal Disk profile Sketch using an Equation-driven curve. . . . .	22
5.1	Experimental setup for precision testing, showing the laser pointer mounted on the prototype stage and the target surface. . . . .	25
5.2	Experimental setup for dynamic torque testing . . . . .	26
5.3	Standard Deviation of Angular Error vs. Microstepping Setting. . . . .	28
5.4	Dynamic error for the Half Step setting, showing highly stable and consistent performance. . . . .	29
5.5	Dynamic error for the 1/32 Step setting, showing a noticeable increase in variability. . . . .	29
5.6	Dynamic error for the 1/64 Step setting, showing a further increase in instability. . . . .	30
6.1	Wear marks observed on the bottom face of the output disk after disassembly, indicating unintended contact with the housing during operation. . . . .	33
8.1	Parametric Equation Driven Curve . . . . .	41
8.2	Initial rough project plan . . . . .	56
8.3	Gantt chart . . . . .	57

# Nomenclature

## Abbreviations

CAL	Computed Axial Lithography
DLP	Digital Light Processing
DMD	Digital Micromirror Device
FDM	Fused Deposition Modeling
FOC	Field-Oriented Control
FOSH	Free and Open-Source Hardware
IC	Integrated Circuit
LED	Light Emitting Diode
MCU	Microcontroller Unit
PETG	Polyethylene Terephthalate Glycol
PID	Proportional-Integral-Derivative
PLA	Polylactic Acid
SLM	Spatial Light Modulator
UART	Universal Asynchronous Receiver/Transmitter
UV	Ultraviolet
VAM	Volumetric Additive Manufacturing

## Roman Symbols

<i>d</i>	Distance from rotation stage to measurement surface	mm
<i>F</i>	Force	N
<i>g</i>	Acceleration due to gravity	m/s <sup>2</sup>
<i>m</i>	Mass	kg
<i>r</i>	Radius or distance from axis of rotation	m
<i>x</i>	Linear displacement on measurement surface	mm

## Greek Symbols

$\theta$	Commanded or theoretical rotation angle	°
$\theta_{\text{actual}}$	Measured actual rotation angle	°
$\tau$	Torque	N·m

## Other Symbols

"	Arcsecond (1/3600 <sup>th</sup> of a degree)
---	--

# Abstract

This project addresses the financial barrier posed by the high cost of a commercial high-precision rotation stage, which often limits their use in research and education. The objective was to design, build, and validate a low-cost, high-torque rotation stage suitable for applications such as Computed Axial Lithography (CAL), 3D scanning, and optical experiments. Developed under Free and Open-Source Hardware (FOSH) principles, all design files and software are publicly available.

The core of the system is a 3D-printed cycloidal drive with a 17:1 reduction ratio, chosen for its high torque output in a compact form. Components were produced using Fused Deposition Modelling (FDM) with PETG. A closed-loop stepper motor (MKS SERVO42D) provides precise motion using encoder feedback to detect and correct positional errors. Control is handled by custom Python code featuring a Graphical-User-Interface(GUI) running on a Raspberry Pi, paired with a CAN bus interface for reliable communication and device management.

Performance testing showed a maximum dynamic output torque of 1.47 Nm, more than three times that of the Thorlabs PRM1Z8 (0.4 Nm). Precision testing demonstrated unidirectional repeatability of approximately  $\pm 0.01$  degrees and an average repeatability of 0.024 degrees. Increasing the microstepping resolution reduced positional stability due to static friction in the drive.

Built for under £250 compared to over £1500 for commercial alternatives, the prototype demonstrates a strong price-to-performance ratio. As a first iteration, it provides a validated and open-source foundation for further development of low-cost, high-precision tools for scientific research.

# Acknowledgements

I would like to express my sincere gratitude to my project supervisor, Nadia Khoura, for their invaluable guidance, encouragement, and insightful feedback throughout the duration of this research. Their expertise and patience were instrumental in navigating the challenges of this project.

My thanks also go to the academic and technical staff at the New Model Institute for Technology and Engineering (NMITE). For their practical assistance and advice.

I would also like to acknowledge the support of my peers in the MEng Integrated Engineering program. The collaborative discussions and shared problem-solving sessions were both helpful and motivating.

Finally, I wish to extend a special thank you to my family and friends for their unwavering support, understanding, and encouragement throughout my studies.

# Chapter 1

## Introduction

### 1.1 Project Background and Objectives

This project builds upon work undertaken during a previous project, which involved modifying a consumer-grade DLP projector for use in Computed Axial Lithography (CAL) [1]. The project focused on replacing the projector's original light source with a high-power ultraviolet (UV) LED, enabling photo-curing of resin volumes using CAL-compatible wavelengths. The aim was to adapt commercially available hardware for research use, thereby reducing the cost of entry into volumetric additive manufacturing [2].

During that project, it became clear that while modifying projection systems could reduce equipment costs, another critical component of the CAL setup, the rotation stage, remained expensive and inaccessible to many. Commercial solutions such as the Thorlabs PRM1Z8 offer the required precision and stability, but their high cost limits their use to well-funded laboratories [3].

This observation led to the conception of the current project: to design and fabricate a low-cost, high-precision rotation stage that replicates the functional capabilities of commercial alternatives, thereby making precision rotational systems for CAL, 3D scanning, and optical experiments more accessible to researchers, educators, and prototyping enthusiasts [4].

#### 1.1.1 Objectives

The main objectives are:

- To design a motorised rotation stage capable of sub-degree angular resolution ( $0.10^\circ$ ) and repeatability.
- To reduce overall system cost by using off-the-shelf mechanical components, 3D printing, and open-source control electronics.
- To ensure compatibility with microcontroller-based platforms for easy integration into custom CAL setups.
- To evaluate the mechanical performance and precision of the stage developed against PRM1Z8.
- To document the design and make it reproducible, contributing to broader accessibility for CAL, 3D scanning, and optical applications.

## 1.2 Problem Significance and Rationale

Computed Axial Lithography (CAL) is a volumetric additive manufacturing technique that relies on accurate angular projection of light to reconstruct three-dimensional geometries within a photosensitive resin. A critical component of this process is the rotation stage, which must enable precise, repeatable angular movement of either the projection system or the target volume. Commercially available rotation stages, such as the Thorlabs PRM1Z8[5], offer sub-degree resolution and reliable performance; however, they are cost-prohibitive for many research groups, educators, and makers [3].

The high cost of such devices presents a barrier to entry, limiting the exploration of CAL and other advanced techniques by those without significant funding or institutional support [6]. Furthermore, the lack of affordable alternatives hinders the decentralisation and democratisation of research in fields like volumetric manufacturing and automated 3D scanning. As these technologies move closer to real-world deployment, the need for accessible and precise rotational hardware becomes increasingly significant.

This project addresses this gap by developing a low-cost alternative to the PRM1Z8 that maintains sufficient performance for CAL applications. In doing so, it contributes toward making CAL more accessible, reproducible, and scalable in academic and prototyping environments [7].

## 1.3 Project Scope

The scope of this project includes the design, development, and testing of a functional, motorised rotation stage prototype. This covers:

- The mechanical design of the stage, including the cycloidal drive mechanism and housing, optimised for Fused Deposition Modelling (FDM) 3D printing.
- The selection and integration of all electronic components, including the stepper motor, closed-loop driver, and control board.
- The development of control software to operate the stage, perform test sequences, and log data.
- The characterisation of the prototype's performance, specifically its positional accuracy, repeatability, backlash, and torque output.

## 1.4 Project Constraints

The project's direction was shaped by four key constraints:

- **Budget:** An initial budget of £150 was set as a soft limit, driving all design choices toward maximum cost-effectiveness.
- **Fabrication:** The use of Fused Deposition Modelling (FDM) 3D printing was a core constraint, chosen to minimise cost while introducing challenges in tolerance and material strength.
- **Components:** All parts had to be readily available off-the-shelf to ensure the design was easily reproducible by others.
- **Open-Source:** The project was constrained by Free and Open-Source Hardware (FOSH) principles, requiring all design files and software to be made publicly available.

\*This project does not encompass the development of a complete CAL printing system, the design of an optical projection system, or the formulation of photosensitive resins. The stage's performance is evaluated on a test bench, not within an active CAL manufacturing process.\*

# Chapter 2

## Background Overview

### 2.1 Introduction

This chapter provides the technical and contextual foundation for the project. It begins by introducing the core application, Computed Axial Lithography (CAL), and establishes the performance requirements for the rotation stage. A review of the key enabling technologies is then presented, including an analysis of drive mechanisms, with a focus on the cycloidal drive, and a detailed comparison of open-loop versus closed-loop stepper motor control. The chapter concludes by discussing common sources of positional error and situating the project within the wider context of the Free and Open-Source Hardware (FOSH) movement.

### 2.2 Computed Axial Lithography (CAL)

Computed Axial Lithography (CAL) is a volumetric additive manufacturing (VAM) technique that fabricates parts by projecting patterns of light into a rotating volume of photosensitive resin. Unlike layer-by-layer methods, CAL forms the entire object simultaneously (or near-simultaneously) through the tomographic superposition of these light patterns[8, 9].

The core principle involves irradiating a photopolymer resin with dynamically varying 2D light patterns from multiple angles as the resin volume rotates. The cumulative light dose at each point is precisely controlled, and when this dose exceeds a certain threshold, the resin cures to form the solid part [8]. Synchronisation between the projected patterns and the vial's angular position is critical for accurate 3D object reconstruction [10]. Table 2.1 outlines the key components of a typical CAL system.

Table 2.1: Key Components of a Typical CAL System.

Component	Primary Function
Light Source	Provides the illumination (e.g., UV LED, laser) required to cure the photosensitive resin.
Spatial Light Modulator (SLM)	Creates the sequence of 2D light patterns that are projected into the resin. A Digital Micromirror Device (DMD) is often used.
Projection Optics	Focuses and directs the 2D patterns from the SLM into the rotating resin volume.
Resin Container	A transparent vial or cuvette that holds the liquid photopolymer resin.
Precision Rotation Stage	Rotates the resin container at a controlled and synchronised speed, enabling the tomographic reconstruction.

#### 2.2.1 Rotation Stage Requirements and Low-Cost Implementations

The rotation stage is a cornerstone of a CAL system, and its performance directly impacts the quality of the final print. Its primary function is to provide smooth, precise, and repeatable angular positioning of the resin vial. This includes high angular resolution, low backlash (lost motion on direction reversal) for bidirectional motion, and minimal wobble or runout to prevent geometric inaccuracies in the printed part [11]. While the qualitative requirements are clear, specific quantitative error budgets are not extensively documented in the literature, so performance targets for low-cost systems are often inferred from the capabilities of commercial stages used in successful CAL research [12, 5].

Published CAL research often employs these high-precision commercial rotation stages [8, 9]. However, efforts to reduce the overall cost of CAL systems have led to a search for more accessible alternatives. Although academic literature lacks examples of low-cost stages specifically validated for CAL, the open-source hardware community provides many general-purpose designs that serve as a foundation for this project [13, 14].

## 2.2.2 Drive Mechanisms for Precision Rotation

The choice of drive mechanism has a significant impact on the performance, size, and cost of a rotation stage. This project focuses on a **cycloidal drive**, a type of compact, high-ratio speed reducer used in many industrial power transmission applications [15, 16]. This epicyclic gear system can achieve high torque ratios in a small space, and its mechanism confers several key advantages, including high shock load absorption and high efficiency [17, 18, 15]. However, its geometry is complex to manufacture, and if tolerances are not tightly controlled, it can exhibit significant backlash [19, 15].

When compared to other high-ratio mechanisms, cycloidal drives present distinct trade-offs. **Harmonic drives**, which are topologically identical, are renowned for providing zero backlash and are ideal for high-precision robotics. In contrast, cycloid drives can be thinner, more efficient (especially at low torques), and have lower reflected inertia, but they inherently exhibit significant backlash [19, 15]. Other alternatives like **worm gears** can also achieve high reduction ratios but typically have lower efficiency and significant backlash unless specifically designed with anti-backlash features [20]. For lower-cost applications, **belt drives** are a popular alternative that can offer very low backlash; the mount by Nilsson et al., for example, minimises backlash by carefully managing belt tension [21]. Finally, while standard **planetary gearboxes** can be efficient, they often require multiple stages to achieve the high ratios possible in a single-stage cycloid drive, which increases size and complexity [17].

## 2.2.3 Bearings for Precision Rotation Stages

Bearings are crucial for supporting the rotating load, ensuring smooth motion, and minimising unwanted play. Key characteristics for this application include low friction, high stiffness, and high precision (low runout), which are defined by standards such as the ABEC tolerance classes [22]. While high-precision angular contact bearings are common in commercial systems, a low-cost design philosophy necessitates alternative solutions. Standard **deep groove ball bearings** are widely available and inexpensive, offering sufficient precision if mounted carefully. Another approach is the use of **partially printed bearings**, where only the races are 3D printed to hold inexpensive rolling elements like steel or plastic balls. This method significantly reduces cost but at the expense of lower inherent precision, making it suitable for low-load applications where cost is the primary driver [23].

## 2.3 Stepper Motor Control

Stepper motors are widely used in precision positioning systems due to their ability to move in discrete, repeatable steps. The most common type for precision applications is the **hybrid stepper**, which combines features of permanent magnet and variable reluctance motors for good torque, speed, and resolution [24]. They operate by energising different sets of coils in sequence to create a rotating magnetic field that the rotor follows.

Although these motors can be driven by advanced open-loop controllers such as the Trinamic TMC2209, which offers quiet operation and smooth motion, such systems share a fundamental limitation [25]. Lacking positional feedback, they cannot detect or correct missed steps caused by high loads or stiction (static friction). This potential for uncorrected cumulative error makes even advanced open-loop systems unsuitable for applications like CAL that demand guaranteed positional accuracy.

### 2.3.1 Closed-Loop Stepper Motor Control for Enhanced Precision

To overcome the inherent limitations of open-loop control, this project explores a closed-loop approach that incorporates positional feedback from a rotary encoder mounted on the motor shaft.

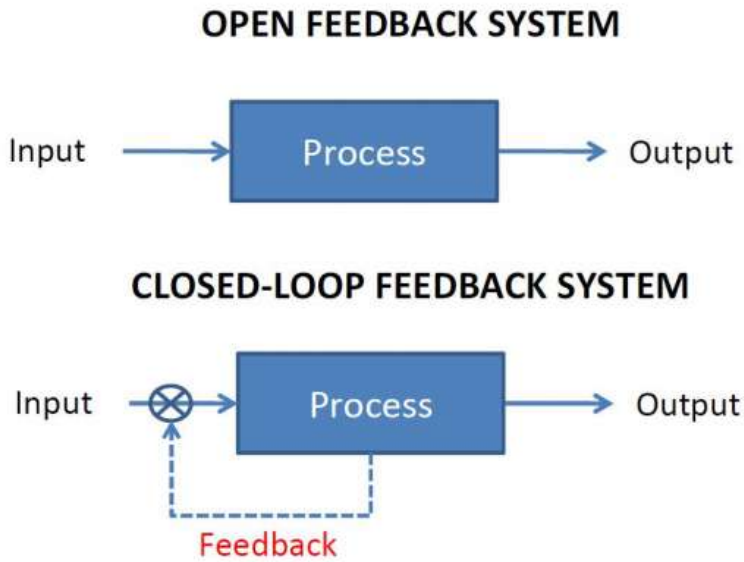


Figure 2.1: A flow diagram of an open loop system vs a Closed loop system [26]

#### Concept and Benefits of Closed-Loop Stepper Systems

In a closed-loop stepper system, an encoder continuously monitors the motor's angular position. This feedback signal is routed to a controller that compares the actual position with the commanded target. If a discrepancy is detected (e.g., from a missed step), the controller can dynamically take corrective action to ensure the target position is accurately reached and maintained [27, 28]. The key benefits of this control topology for precision motion applications are well established and are summarised in Table 2.2.

Table 2.2: Key Benefits of Closed-Loop Stepper Motor Control.

Benefit	Description
<b>Error Detection &amp; Correction</b>	The system actively works to prevent step loss. This correction of position error is a primary advantage over open-loop systems for improving both absolute positional accuracy and long-term repeatability [29, 27].
<b>Improved Dynamic Performance</b>	By monitoring the rotor's true position, the controller can handle varying loads and rapid accelerations more effectively, making the system more robust and responsive [28].
<b>Higher Efficiency &amp; Reduced Heat</b>	Motor current is optimised based on actual load requirements rather than being set at a constant high value, leading to significant reductions in motor heating and overall energy consumption [27].
<b>Stall Prevention</b>	The system can detect an impending stall condition and apply more torque or alert the host system, leading to more robust and reliable operation under challenging or unpredictable loads [29, 28].

## Integrated Closed-Loop Stepper Systems (e.g., MKS SERVO42D)

Although it is feasible to construct a custom closed-loop system by pairing a standard stepper motor with an external encoder and developing the necessary control algorithms, several manufacturers now offer integrated "closed-loop stepper" or "easy-servo" motor solutions. The Makerbase (MKS) SERVO42D, chosen for this project, is an example of such an integrated system [30]. These units typically comprise:

- A NEMA 17 stepper motor as the actuator.
- An integrated high-resolution rotary encoder. For instance, the MKS SERVO42D employs a 14-bit magnetic encoder, offering  $2^{14} = 16,384$  counts per revolution. This translates to a raw angular resolution of approximately  $360^\circ / 16,384 \approx 0.022^\circ$  from the encoder itself [30].
- A dedicated driver board, often mounted directly to the rear of the motor. This board includes a microcontroller (e.g., an ARM Cortex-M series MCU), gate drivers, and power MOSFETs to manage the closed-loop control in real-time [30].

These integrated systems frequently employ advanced control strategies such as **Field-Oriented Control (FOC)**. FOC is a motor control technique that provides smooth, quiet operation with precise torque control by independently controlling the motor's flux and torque-producing currents, similar to high-performance AC servo drives [31]. A **Proportional Integral Derivative (PID)** control loop is also typically implemented within the onboard microcontroller to manage the motor position and velocity, ensuring rapid and accurate response to commands and effective management of disturbances [32].

## Interface, Configuration, and Implications

Integrated closed-loop stepper systems like the MKS SERVO42D are designed for ease of integration. They often accept standard STEP/DIR input signals for drop-in compatibility with existing motion controllers, while also providing advanced serial interfaces (e.g., UART, RS485, or CAN bus). These serial connections allow for initial parameter configuration, real-time diagnostics, and direct control over the motor's position, velocity, or torque, offering more sophisticated capabilities than STEP/DIR signals alone [30].

For a precision rotation stage intended for demanding applications like CAL, the implications of this control method are significant. The primary advantage is guaranteed positional accuracy and high repeatability, as the encoder feedback actively prevents and corrects for step loss [27]. This ensures robust performance even under the varying dynamic loads and friction present in a geared system. Furthermore, the use of control algorithms like FOC results in exceptionally smooth and quiet motor operation, which is critical for minimising vibrations in sensitive optical setups [31].

The main trade-offs when selecting such a system are a higher unit cost compared to open-loop components and a potentially more involved initial setup. However, many integrated units come with robust, pre-tuned parameters and clear documentation, mitigating the complexity of implementation.

### 2.3.2 Comparison of Control Strategies

The selection between an advanced open-loop and an integrated closed-loop system determines how effectively these positional errors are managed. The choice involves clear trade-offs in performance, complexity, and cost, as summarised in Table 2.3.

Table 2.3: Comparison of Closed-Loop and Advanced Open-Loop Control Systems.

Criterion	Closed-Loop System (e.g., MKS SERVO42D)	Advanced Open-Loop System (e.g., TMC2209)
<b>Positional Accuracy &amp; Repeatability</b>	<b>High.</b> Guarantees final position by actively correcting missed steps via encoder feedback; the key advantage for precision work [33].	<b>Moderate.</b> Susceptible to uncorrected errors from missed steps. Lacks a feedback mechanism to confirm position.
<b>Response to Load Variations</b>	<b>Robust.</b> Dynamically compensates for load variations to maintain commanded motion [27].	<b>Vulnerable.</b> Loses steps if disturbance torque exceeds holding torque.
<b>Motion Smoothness</b>	<b>Excellent.</b> Control strategies like FOC provide smooth, high-torque rotation, especially at low speeds.	<b>Very Good.</b> Microstepping provides smooth motion, but can suffer from torque ripple.
<b>Error Handling</b>	<b>Inherent.</b> Can overcome stiction (static friction) with torque control. Ensures motor shaft position but cannot fix downstream gearbox backlash [29].	<b>Limited.</b> Cannot compensate for backlash or stiction (static friction), leading to lost motion.
<b>System Complexity &amp; Cost</b>	<b>Higher.</b> Higher unit cost and more complex configuration, but offloads real-time control from the host MCU.	<b>Lower.</b> Lower component cost and simpler hardware setup.

Given the project's objective to develop a *high-precision* stage where angular accuracy is crucial, the comparison justifies the selection of a closed-loop system. The assurance of not losing steps under the potentially varying loads of a cycloidal drive outweighs the lower cost of an open-loop alternative.

## 2.4 Backlash and Positional Error

Accurate positioning is paramount in CAL, as various mechanical errors, defined in Table 2.4, contribute to deviations from the desired position. These errors primarily arise from manufacturing tolerances, component misalignments, wear, and deflection under load.

Table 2.4: Common Positional Errors in Motion Systems.

Term	Definition
<b>Backlash</b>	Lost motion or "play" in a mechanism when movement is reversed, typically caused by clearance between gear teeth [11].
<b>Hysteresis</b>	The difference in achieved position when approaching a target from opposite directions, encompassing backlash, friction, and material flex [11, 34].
<b>Runout</b>	The total deviation from a true circular path as a component rotates, measured either radially (side-to-side) or axially (wobble) [11].
<b>Positional Accuracy</b>	The maximum deviation between the stage's commanded position and the actual position it achieves [11].
<b>Repeatability</b>	The ability of the stage to return to the same commanded position multiple times under identical conditions [11].

### 2.4.1 Impact, Measurement, and Mitigation

In CAL, uncompensated positional errors directly impact print quality, leading to geometric distortions, loss of resolution, and surface artefacts [10]. The management of these errors involves a combination of strategies. Key errors like backlash and runout can be **measured** using tools like dial indicators.

More importantly, they can be **minimised** at the design stage through anti-backlash gears, careful bearing selection, and ensuring the structural stiffness of 3D-printed parts. Finally, software **compensation** can be used to correct for known, repeatable errors, though this adds complexity to the control system [35].

## 2.5 Low-Cost and Open-Source Scientific Hardware

This project is situated within a growing movement in the scientific community to develop low-cost, accessible research tools using open-source principles and digital fabrication.

### 2.5.1 Precedent in 3D-Printed Optical Mounts

The high cost of commercial optical components, such as motorised rotation mounts, often limits their use in research and educational settings [21]. A commercial motorised rotation stage can cost upwards of £1,850, a price point that discourages widespread adoption and experimentation [21]. In response, there has been a growing movement to leverage the accessibility of 3D printing and low-cost electronics to develop open-source laboratory equipment [21].

Nilsson et al. demonstrated the viability of this approach by designing, building, and validating two types of 3D-printed motorised rotation mounts for 1-inch optics [21]. Their work provides a step-by-step guide showing that it is possible to build mounts for less than \$220 that perform similarly to expensive commercial systems in key metrics like velocity, precision, and backlash [21].

Their design philosophy, which constrains the budget and uses a combination of 3D-printed parts and readily available off-the-shelf components, aligns closely with the objectives of this project. This reinforces the feasibility of creating affordable, high-performance mechatronics for optical applications and provides a benchmark for evaluating the success of the low-cost rotation stage developed.

### 2.5.2 FOSH Case Studies and Design Philosophy

Numerous projects show that sophisticated scientific instruments can be created at significantly reduced costs using accessible technologies like 3D printing and microcontrollers. Examples include low-cost microplate readers and open-source microscopy platforms such as the OpenFlexure microscope system, which uses a high-precision, 3D-printed translation stage [36, 37]. The design philosophy of Free and Open-Source Hardware (FOSH) often emphasises modularity, customisability, and community-driven development [38].

Key principles in FOSH design include [38]:

- Prioritising accessibility and affordability without critically compromising essential functionality.
- Utilising digital fabrication (3D printing, laser cutting) for custom parts.
- Employing open-source software and controllers.
- Extensive documentation to enable replication and modification.

### 2.5.3 Impact on Research Accessibility

Low-cost mechatronics and FOSH lower the barrier to entry for researchers in underfunded institutions, educational settings, and citizen science initiatives. They enable greater customisation of tools to specific research needs and foster collaboration and innovation [38]. However, challenges include ensuring quality control, providing user support, and overcoming perceptions about the reliability of non-commercial instruments.

## 2.6 Informal Sources and Community Knowledge

Beyond formal academic literature, a wealth of practical knowledge for developing low-cost mechatronic systems resides in informal sources:

- **Maker Communities and Forums:** Websites like Hackaday, Instructables, Thingiverse, and various robotics/CNC forums host numerous DIY projects related to precision rotation stages, offering practical tips and community-vetted designs.
- **Open-Source Project Repositories (e.g., GitHub):** Provide direct access to design files, source code, and documentation for a wide range of relevant hardware projects.
- **Blogs and YouTube Channels:** Many engineers and hobbyists share detailed build logs, tutorials, and performance analyses of their DIY mechatronic devices.

While these informal sources may lack the rigorous peer review of academic publications, they proved invaluable for this project. They offer a wealth of practical implementation tips, community-vetted designs, and troubleshooting advice that is often not present in formal literature, providing a crucial knowledge base for hands-on hardware development.

### 2.6.1 Cycloidal Drive Design

The design of a functional 3D printed cycloidal drive is a well-documented topic within open-source hardware and engineering communities, with numerous tutorials providing insights into the specific challenges of FDM fabrication. Successful designs, such as those demonstrated by [39] and [40], invariably rely on parametric CAD software to model the complex geometry of the cycloidal disk and the corresponding ring gear pins.

This approach not only allows for the easy adjustment of key parameters like the gear reduction ratio but also facilitates the critical step of implementing printer-specific tolerances and compensations (e.g., horizontal expansion in the slicer) to ensure a smooth, low-friction fit between moving parts. These community-led projects provide an invaluable practical knowledge base for achieving the precision required from what are otherwise difficult-to-manufacture components.

### Summary of Background Overview

This chapter provides a technical background overview, establishing the context and theoretical foundation for the project. It begins by defining **Computed Axial Lithography (CAL)**, highlighting the critical role of a precision rotation stage and the prohibitive cost of commercial options, which justifies the need for a low-cost alternative.

The overview then examines the core technologies required to build such a stage. It analyses various **drive mechanisms**, selecting the high-torque **cycloidal drive** and comparing it to alternatives such as harmonic and worm gears. It covers different **stepper motor control** strategies, contrasting the limitations of open-loop systems with the superior accuracy and reliability of the **closed-loop control** chosen for this project.

Finally, this chapter discusses key engineering challenges, including sources of **positional error** like backlash and runout, and places the project within the wider context of the **Free and Open-Source Hardware (FOSH)** movement, which aims to democratise scientific tools.

# Chapter 3

## Methodology

### 3.1 Introduction

Having established the technical background and identified the project's core challenges in the previous chapter, this chapter outlines the methodology used to systematically progress from concept to a validated prototype. It details the **Hybrid Methodology**, a blend of a formal Stage-Gate model and an Iterative Design cycle, chosen to balance structured planning with the flexibility needed for hardware development. The chapter also presents the initial risk assessment of the project and describes the five distinct stages of work, from research and planning through to the final validation of the performance.

### 3.2 Methodological Framework

Developing a novel mechatronic system from concept to prototype required a framework providing both high-level project governance and flexibility. This project adopted a Hybrid Methodology, combining the structured, sequential phases of a formal Stage-Gate model with the adaptability of an Iterative Design cycle for hands-on hardware development.

A rigid, linear framework like the Waterfall model was considered inappropriate for the project, as it fails to account for the empirical discovery required during hardware prototyping. Conversely, a purely agile framework would lack the formal structure needed for the initial research and planning stages, where clear, sequential deliverables are necessary.

The chosen hybrid model leverages the strengths of both approaches: structured planning for predictable phases and iterative problem-solving for the uncertain prototyping phase. An initial project schedule was developed using a Gantt chart (see Appendix figs. 8.2 and 8.3) to guide these structured phases. While the actual project timeline deviated from this initial plan, as is common in research and development, the chart served as a crucial baseline for tracking progress and managing deliverables. This approach directly addressed the requirement to navigate uncertainty with informed decision-making.

### 3.3 Project Management and Risk Assessment

Effective project management requires not only planning the stages of work but also anticipating and mitigating potential risks. A risk assessment was conducted at the outset to identify key technical and logistical challenges. The primary risks and their mitigation strategies are summarised in Table 3.1. This approach informed key methodological decisions, such as the adoption of an iterative cycle to specifically address the high-risk nature of fabricating precision components with FDM printing.

Table 3.1: Project Risk Assessment and Mitigation Strategies.

Risk Description	Likelihood	Impact	Mitigation Strategy
<b>Technical Risks</b>			
Manufacturing tolerances of FDM printing are insufficient for the smooth operation of the cycloidal drive, causing high friction or jamming.	High	High	Adopt an iterative design-print-test cycle. Design components parametrically in CAD to allow for rapid adjustments to clearances and tolerances.
The closed-loop stepper motor (MKS SERVO42D) does not perform as expected or presents complex integration challenges.	Medium	High	Select a motor with comprehensive documentation and community support. Allocate specific time for software integration and testing before final assembly.
Structural failure of 3D-printed PETG components under maximum torque load.	Low	Medium	Use conservative design principles (e.g., thicker walls, higher infill) for load-bearing parts. Conduct a destructive torque test to find the system's true failure point.
<b>Logistical Risks</b>			
Delays in component delivery (motor, electronics) impact the project timeline.	Medium	Medium	Order all critical, long-lead-time components at the very start of the project. Identify alternative suppliers where possible.
Significant time was lost due to failures in the 3D printing process (e.g., failed prints, machine maintenance).	Medium	Low	Schedule buffer time for fabrication. Maintain the 3D printer regularly and use reliable, pre-tested print settings.

The application of these mitigation strategies significantly reduces the project's overall risk profile. As the post-mitigation assessment in Table 3.2 illustrates, the likelihood of most challenges occurring has been lowered to a manageable level.

Table 3.2: Project Risk Assessment After Mitigation.

Risk Description	Likelihood	Impact	Rationale for Change
<b>Technical Risks</b>			
Manufacturing tolerances of FDM printing are insufficient for the smooth operation of the cycloidal drive, causing high friction or jamming.	Low	High	The iterative design-print-test cycle significantly lowers the probability of final failure, although the impact, should it still occur, remains high.
The closed-loop stepper motor (MKS SERVO42D) does not perform as expected or presents complex integration challenges.	Low	Medium	Selecting a well-documented motor and allocating specific integration time reduces the likelihood of unforeseen issues and lessens their impact on the overall project timeline.
Structural failure of 3D-printed PETG components under maximum torque load.	Low	Medium	The risk was already low. Using conservative design principles and conducting destructive testing further reduces the likelihood of failure to a minimal level.
<b>Logistical Risks</b>			
Delays in component delivery (motor, electronics) impact the project timeline.	Low	Medium	Ordering critical components early and identifying backups makes it much less likely that supplier delays will affect the project's critical path.
Significant time was lost due to failures in the 3D printing process (e.g., failed prints, machine maintenance).	Low	Low	Regular maintenance and tested settings reduce the frequency of print failures, while scheduled buffer time minimizes the impact of any failures that do occur.

### 3.4 The Stage-Gate Model

The Stage-Gate model is a project management framework that divides a project into a series of discrete stages, separated by decision points known as "gates" [41]. At each gate, the project is evaluated against a set of predetermined criteria. A decision is then made to either continue investment and proceed to the next stage, pivot the project's direction, or halt the project entirely. This structured process provides clear points for review and ensures that resources are committed only to projects that remain technically feasible and aligned with their original objectives.

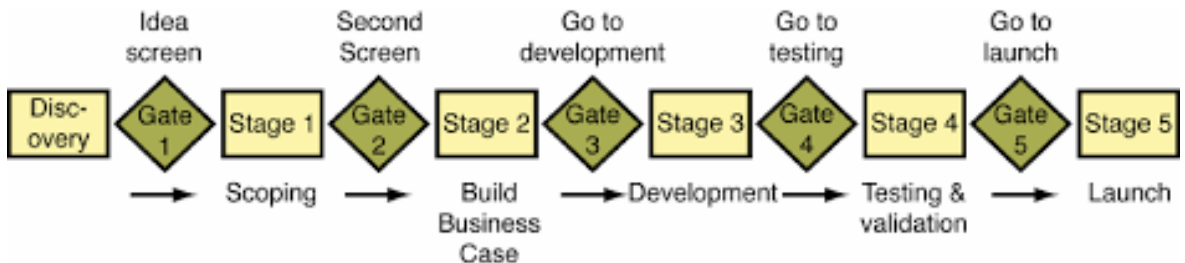


Figure 3.1: An Example of a typical Stage gate process [42].

### 3.5 The Iterative Design Process

Iterative design is a cyclical process of prototyping, testing, analysing, and refining a product or system. Unlike a linear process where each phase is completed once, an iterative cycle repeats these steps, allowing for the continuous improvement of a design based on feedback and empirical testing [43].

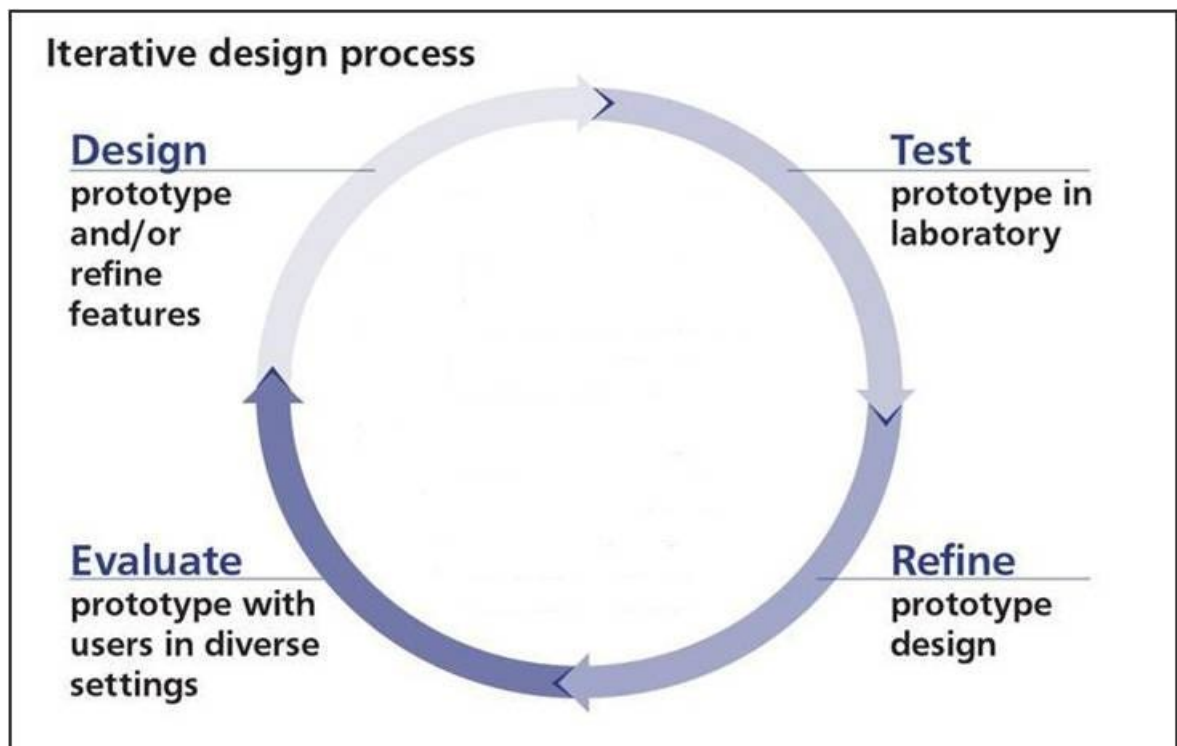


Figure 3.2: An example of a typical Iterative Design Cycle [44].

This approach is particularly well-suited for projects with a high degree of uncertainty, as it allows developers to identify and solve unforeseen problems through repeated, hands-on experimentation. For this project, the iterative cycle was primarily used in Stage 3 to refine the mechanical hardware.

## 3.6 Application of the Stage-Gate Model

### Stage 1: Research and Planning

The initial phase followed a sequential process, beginning with a comprehensive literature review to establish a theoretical foundation. This research directly informed the definition of the project's scope, objectives, and key design constraints. Preliminary CAD models were created to verify component fit and layout. *Gate 1: The decision to proceed was based on a feasible concept and a clear set of performance targets.*

### Stage 2: System Design and Component Selection

Following the approval at Gate 1, the detailed design phase began. Key components like the MKS SERVO42D controller and PETG structural material were selected. The rotation stage was then designed in detail using CAD software, culminating in a complete digital assembly model. *Gate 2: The decision to commit resources to fabrication was based on a complete and validated digital design.*

### Stage 3: Prototyping and Iteration

This stage marked a deliberate shift to an Iterative Design methodology. The process of creating a functional hardware prototype involved repeated cycles of fabrication, assembly, and evaluation. Issues identified during hands-on testing—such as insufficient gear engagement, shaft misalignment, and excessive friction—were addressed by specific modifications to the CAD model until a mechanically stable prototype was achieved. *Gate 3: The decision to move to software development was based on achieving a mechanically robust and functional prototype.*

### Stage 4: Coding and Troubleshooting

With a working hardware platform from Stage 3, this phase focused on software development and system integration. The control software and Graphical User Interface (GUI) were developed in Python. This involved significant troubleshooting to establish reliable CAN bus communication and to calibrate the motor's command and feedback signals.

*Gate 4: The decision to proceed to final validation was based on demonstrating stable and reliable control of the hardware via the custom software.*

### Stage 5: Performance Validation

With a fully controlled prototype approved at Gate 4, the final stage focused on formal performance validation. A predefined test plan was executed to characterise the prototype's positional accuracy, repeatability, and output torque against the objectives established in Stage 1. The project concluded with the analysis of the test data and the compilation of this report.

## 3.7 Summary of Methodological Approach

This chapter details the project's methodological framework, which was designed to balance formal project governance with the flexibility required for hardware development. A **Hybrid Methodology** was adopted, combining a structured, five-stage **Stage-Gate model** with an **Iterative Design cycle** for the hands-on prototyping phase. An initial risk assessment was conducted to identify and mitigate key technical challenges. The project progressed through five distinct stages: 1) Research and Planning, 2) System Design, 3) Prototyping and Iteration, 4) Coding and Troubleshooting, and 5) Performance Validation, with specific deliverables required to pass through each gate.

# Chapter 4

# System Design and Development

## 4.1 Introduction

This chapter presents the technical outcomes of the design and development process outlined in the Methodology. It details the final **component and material selection**, and provides a breakdown of the core **mechanical design**, including the governing equations and parameters for the custom cycloidal drive. The chapter concludes by describing the architecture and implementation of the Python-based **control software** and its Graphical User Interface (GUI).

## 4.2 Component and Material Selection

With the initial research complete, components were selected to balance performance, cost, and ease of integration, in line with the project's objectives. A NEMA 17 stepper motor was selected as the core actuator for its low cost and wide commercial availability. To meet the precision requirements established in the Background Overview, and following the comparison of control strategies in Section 2.3.2, the MKS SERVO42D integrated closed-loop system was selected [30], as it combines the motor with a high-resolution encoder, FOC control, and a CAN bus interface. A Raspberry Pi 4 was chosen as the host microcontroller due to its processing power and extensive Python library support.

A combination of standard and custom-fabricated bearings was used for the mechanical components to balance cost and performance. The design primarily utilises **partially-printed bearings** for most low-speed components, including the main output stage. Standard deep groove ball bearings were reserved for critical high-load parts, such as the roller and output pins within the cycloidal drive. For all other structural components, PETG was the primary material, chosen for its superior strength and stability in FDM printing compared to PLA [45], which was used only for non-functional fit checks.

## 4.3 Mechanical Design

### 4.3.1 Cycloidal Drive Design and Parameters

The core of the rotation stage is a cycloidal drive, chosen for its ability to provide a high reduction ratio in a compact form factor. The drive was designed parametrically in CAD software, allowing for precise control over its geometry and performance characteristics.

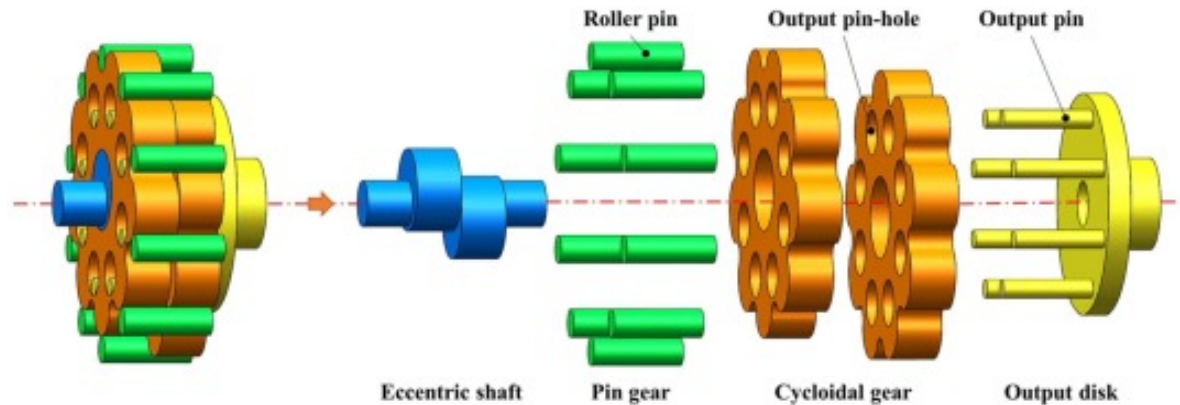


Figure 4.1: An illustration showing the components of a Cycloidal Drive [46].

## Design Constraints

The selection of the design parameters detailed in Table 4.1 was governed by several critical geometric constraints to ensure the drive would operate without interference or jamming. A primary constraint, as identified by Shin & Kwon (2006) [18], relates the cam eccentricity ( $e$ ), the roller pitch radius ( $R$ ), and the number of rollers ( $N$ , or  $Z_2$ ), which must satisfy the condition:  $e < R/N$ . The final parameters were chosen to satisfy this and other geometric conditions, ensuring a valid drive profile.

## Governing Equations

The complex profile of the cycloid disk's lobes was generated using the established trochoidal parametric equations, as described by Shin & Kwon (2006) [18] and Sensinger (2010) [15].

The Cartesian coordinates of the profile,  $(C_x, C_y)$ , are defined as a function of the input angle  $\phi$ :

$$C_x = R \cos(\phi) - R_r \cos(\phi + \psi) - e \cos((Z_1 + 1)\phi) \quad (4.1)$$

$$C_y = -R \sin(\phi) + R_r \sin(\phi + \psi) + e \sin((Z_1 + 1)\phi) \quad (4.2)$$

Where  $\psi$  is the contact angle between the cycloid lobe and a roller, calculated as:

$$\psi = \arctan \left[ \frac{\sin(Z_1\phi)}{\cos(Z_1\phi) - \frac{R}{e(Z_1+1)}} \right]$$

## Design Parameters

The performance and geometry of the drive are determined by a set of key parameters, detailed in Table 4.1.

Table 4.1: Key Design Parameters of the Cycloidal Drive Prototype.

Parameter	Symbol	Value
Number of Cycloid Lobes	$Z_1$	17
Number of Housing Rollers	$Z_2$	18
Roller Pitch Radius	$R$	50 mm
Roller Radius	$R_r$	3.5 mm
Input Cam Eccentricity	$e$	2.5 mm

Based on the chosen parameters, the drive has a reduction ratio of 17:1.

### 4.3.2 CAD Implementation and Prototyping

These parameters and equations were implemented in CAD software using the "Equation Driven Curve" feature to generate the precise 2D sketch of the cycloid disk profile[39, 40]. The exact parametric equations entered into the software can be found in Appendix 8.2.

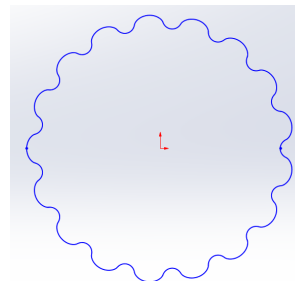


Figure 4.2: Cycloidal Disk profile Sketch using an Equation-driven curve.

## 4.4 Control Software Development

The control software for the rotation stage was developed in Python 3 to provide a robust and user-friendly method for operating the prototype and conducting performance tests. The software utilises a dedicated CAN bus library (`mks-servo-can` built on `python-can`) to interface with the MKS SERVO42D motor, while a Graphical User Interface (GUI) for real-time control was created using Python's standard `Tkinter` library.

### 4.4.1 System Architecture and Design

To ensure the user interface remained responsive during active communication with the motor, a multi-threaded architecture was employed. The software's architecture is designed around two primary threads:

1. **Main Thread:** Manages the Tkinter GUI, handling all user inputs from buttons, entry fields, and drop-down menus.
2. **Background Feedback Thread:** Runs in a continuous loop, responsible for periodically polling the servo's status via the CAN bus. Its sole purpose is to read the current encoder position and post the updated value to the GUI.

This concurrent design prevents the user interface from freezing while waiting for hardware responses, which is critical for providing a smooth user experience and enabling real-time features like the emergency stop. Communication between the background thread and the GUI is handled safely using the `root.after()` method to prevent race conditions.

### 4.4.2 Motion Command and Control Logic

Translating a high-level user request, such as "move to 90.0°," into a low-level motor command involves a precise calculation within the `_set_output_angle.command` function:

1. **Output to Motor Angle Conversion:** The desired output angle, specified in degrees, is first multiplied by the system's `GEAR_RATIO` (17:1) to determine the required rotation of the motor shaft itself.
2. **Angle to Pulse Conversion:** This motor angle is then converted into a discrete pulse value that the servo controller can understand. This calculation is based on the motor's command resolution, defined in the script as `PULSES_PER_MOTOR_REVOLUTION_FOR_COMMAND` (16,384 pulses). The final value represents an absolute position within the motor's internal coordinate system.
3. **Command Transmission:** The final pulse value, along with user-defined speed and acceleration parameters from the GUI, is packaged and sent to the servo over the CAN bus using the `run_motor_absolute_motion_by_axis` command. Input validation is performed before transmission to ensure all parameters are within the servo's operational limits.

### 4.4.3 Position Feedback and Calibration

To provide the user with accurate, real-time positional data, the background thread continuously queries the motor's encoder. The raw data returned by the servo does not directly correspond to a physical angle and must be calibrated and scaled:

- **Calibration Map:** A CALIBRATION\_FEEDBACK\_MAP dictionary was implemented. This map contains scaling factors derived from empirical testing for each of the motor's available microstepping (subdivision) modes. Different modes alter the units of the feedback signal, and this map allows the software to adapt.
- **Feedback Calculation:** The feedback loop first subtracts a stored "zero offset" from the current raw encoder reading. It then uses the appropriate scaling factor from the calibration map to convert this relative raw value into motor degrees. Finally, this value is divided by the GEAR\_RATIO to display the final, true output angle of the stage.

### 4.4.4 Zero Point Synchronisation

A critical function of the software is establishing a zero-reference point. The "Set Zero" function (`on_set_zero_button`) synchronises the software's display with the servo's internal coordinate system in a two-step process:

1. **Command Internal Zero:** A `set_current_axis_to_zero` command is sent to the servo. This instructs the motor controller to treat its current physical position as its new internal origin (i.e., pulse count "0").
2. **Capture Display Offset:** The software immediately reads the encoder's new raw value and stores it as a display offset (`library_feedback_raw_offset_at_zero`). All subsequent angle readings displayed in the GUI are calculated relative to this stored offset.

This two-step process ensures that the user display and the servo's internal logic are perfectly aligned, so that a command to move to "0.0°" will return the stage to the exact position where the zero point was set.

### 4.4.5 Safety and Usability

The software includes an emergency stop (`on_emergency_stop_button`) that immediately halts all motor functions via a dedicated CAN command. Upon activation, all motion and configuration controls in the GUI are disabled to prevent accidental commands from being sent. The full, commented source code for the control software is included in Appendix 8.1 to ensure full reproducibility, in line with the project's open-source hardware goals.

# Chapter 5

## Testing and Results

### 5.1 Precision Testing

This chapter details the quantitative tests conducted to characterise the prototype's performance in its two primary design areas: **positional precision** and **output torque**. The experimental methodologies are described, and the results are presented and analysed against the project's objectives.

A simple optical lever system was established to quantitatively assess the prototype's positional accuracy and repeatability. A laser pointer was mounted securely to the stage's rotating platform, projecting a beam onto a flat target surface (a whiteboard) positioned perpendicular to the beam. The distance ( $d$ ) from the stage's axis of rotation to the target was 2.0 metres.



Figure 5.1: Experimental setup for precision testing, showing the laser pointer mounted on the prototype stage and the target surface.

The testing procedure began by marking the initial position of the laser spot on the target with a whiteboard pen. The stage was commanded to rotate by a specific angle ( $\theta$ ). Once the movement was complete, the new position of the laser spot was marked. The linear displacement ( $x$ ) between the initial and final marks was then measured using digital callipers.

This empirical measurement ( $x_{\text{measured}}$ ) formed the basis for calculating the true angular position of the stage. The measured displacement was then compared to the theoretical displacement calculated using the trigonometric relation:

$$x = d \cdot \tan(\theta)$$

Where:

- $x$  is the linear displacement on the whiteboard (mm),
- $d$  is the distance from the stage to the whiteboard (mm),
- $\theta$  is the commanded rotation angle in degrees.

After measuring the displacement, the actual angle of rotation was determined by rearranging the above relation:

$$\theta_{\text{actual}} = \tan^{-1} \left( \frac{x_{\text{measured}}}{d} \right)$$

This allowed for a direct comparison between the commanded angle and the actual angle achieved by the stage. The difference between these two values was recorded as the angular positioning error, which serves as a quantitative measure of the accuracy of the system. To further assess performance, tests were repeated multiple times at each target angle under the same conditions to evaluate trends such as systematic deviation (bias) and repeatability. A summary of results is provided in Section 5.3, and all raw measurements are available in Appendix 8.3.

### 5.1.1 Repeatability and Backlash

Repeatability was implicitly assessed by multiple repetitions performed during precision testing. For each commanded angle, several identical motions were performed under consistent conditions. The resulting variation in measured displacement and the actual calculated angle provided a practical estimate of the repeatability of the system.

Backlash was not formally isolated as a stand-alone test, but return-to-zero behaviour was monitored qualitatively. Movements approaching  $0^\circ$  from both the clockwise and counterclockwise directions were observed to result in consistent laser positions within the measurement resolution, indicating minimal detectable backlash under the tested conditions. A more rigorous evaluation could be performed in future by explicitly commanding and logging bidirectional offsets.

Across its primary operating range (from full steps to 1/64 microstepping), the prototype demonstrated an average unidirectional repeatability of  $0.024^\circ$ , with optimal performance observed at half-step and quarter-step resolutions.

## 5.2 Output Torque

### 5.2.1 Dynamic Load Performance

Dynamic load performance was evaluated by securing the rotation stage in a bench vice to ensure it remained stationary during testing. A 0.39m torque arm was attached to the output shaft. Calibrated masses were suspended 0.3m away from the centre of the output and increased in 100 g increments, and after each addition, the motor was commanded to rotate  $90^\circ$  upwards to lift the load.



Figure 5.2: Experimental setup for dynamic torque testing

The test aimed to identify the maximum torque the system could produce before stalling or losing steps. Successful completion of the  $90^\circ$  movement indicated that the applied torque was within the system's dynamic load capacity. The applied torque was calculated using the following.

$$\tau = r \cdot F = r \cdot (m \cdot g)$$

Where:

- $\tau$  is the torque in N·m,
- $r = 0.30\text{ m}$  is the distance from the axis of rotation,
- $m$  is the suspended mass in kg,
- $g = 9.81\text{ m/s}^2$  is the acceleration due to gravity.

The key results of this test are summarised in Table 5.1.

Table 5.1: Summary of Dynamic Torque Test Results.

Mass (g)	Mass (kg)	Applied Torque (Nm)	Result
100	0.1	0.29	Success
200	0.2	0.59	Success
300	0.3	0.88	Success
400	0.4	1.18	Success
<b>500</b>	<b>0.5</b>	<b>1.47</b>	<b>Success</b>
600	0.6	1.77	Failure

As shown in Table 5.1, the prototype lifted all loads to and including 500 g. The system failed to complete the rotation when the load was increased to 600 g. The maximum measured output torque was therefore 1.47 Nm.

## 5.3 Analysis of Results

### 5.3.1 Precision Testing

#### Influence of Microstepping on Precision and Repeatability

Microstepping is an electronic technique used to increase the theoretical positioning resolution of a stepper motor by dividing its 1.8° full steps into much smaller increments.

Table 5.2: Theoretical Angular Resolution by Microstepping Setting for a 1.8° Motor.

Setting	Divisions (N)	Steps per Revolution	Resolution (°)	Resolution (arcsec)
Full Step	1	200	1.800000	6480.0
Half Step (1/2)	2	400	0.900000	3240.0
Quarter Step (1/4)	4	800	0.450000	1620.0
1/8 Steps	8	1,600	0.225000	810.0
1/16 Steps	16	3,200	0.112500	405.0
1/32 Steps	32	6,400	0.056250	202.5
1/64 Steps	64	12,800	0.028125	101.3
1/128 Steps	128	25,600	0.014063	50.6
1/256 Steps	256	51,200	0.007031	25.3

As shown in Table 5.2, increasing the microstep divisions from full-stepping to 1/256-stepping theoretically improves the angular resolution by a factor of 256, from 1.8° down to approximately 0.007° (25.3 arcseconds).

A key finding of this project is that this theoretical increase in resolution does not translate to improved practical performance. The experimental results demonstrate a clear inverse relationship between the selected microstepping resolution and the positional consistency of the system.

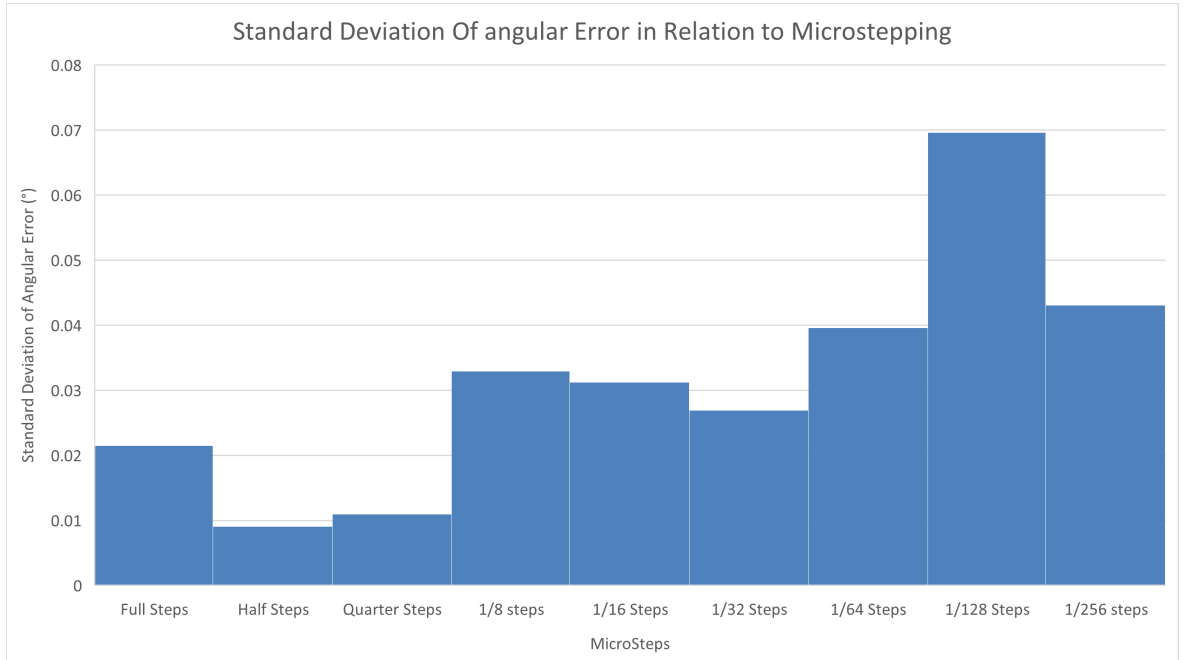


Figure 5.3: Standard Deviation of Angular Error vs. Microstepping Setting.

*Note:* The error variability is lowest for Half and Quarter step modes and increases significantly for finer microstep resolutions.

The relationship between microstep resolution and positional consistency is summarised in Figure 5.3. The data indicates that the highest resolutions do not yield the best performance, with optimal consistency found at the half-step and quarter-step settings. As the resolution increased beyond 1/8 steps, performance degraded significantly, with the 1/128 setting exhibiting the most error variability.

The non-monotonic nature of this degradation, evidenced by the improved performance at 1/256 steps relative to 1/128, points towards complex system dynamics, possibly including motor resonance, which could be a topic for future investigation.

To provide a deeper qualitative understanding of this trend, the dynamic error profiles of three representative settings were analysed. Figure 5.4 establishes a baseline of optimal performance, where the Half Step mode exhibits very low and stable error deviation across the full range of motion. In contrast, Figure 5.5 and Figure 5.6 show a clear, progressive degradation in stability as the microstepping resolution increases.

### 5.3.2 Defining an Acceptable Error Benchmark

To provide a quantitative benchmark for performance across all tests, an acceptable error threshold was established. A relative limit of 10% of the commanded angle was chosen as a practical standard for acceptable error. Then, this criterion was applied to the smallest reliable incremental angle the prototype could consistently achieve, which was determined to be  $0.09^\circ$ . This resulted in the calculation of a fixed, absolute error threshold:

$$0.09^\circ \text{ (Minimum Reliable Step)} \times 10\% = 0.009^\circ$$

This value of  $\pm 0.009^\circ$  was subsequently used as a consistent performance benchmark across all test configurations and commanded angles. Any measurement falling outside this range was considered a significant deviation, allowing for a clear, comparative analysis of the system's stability.

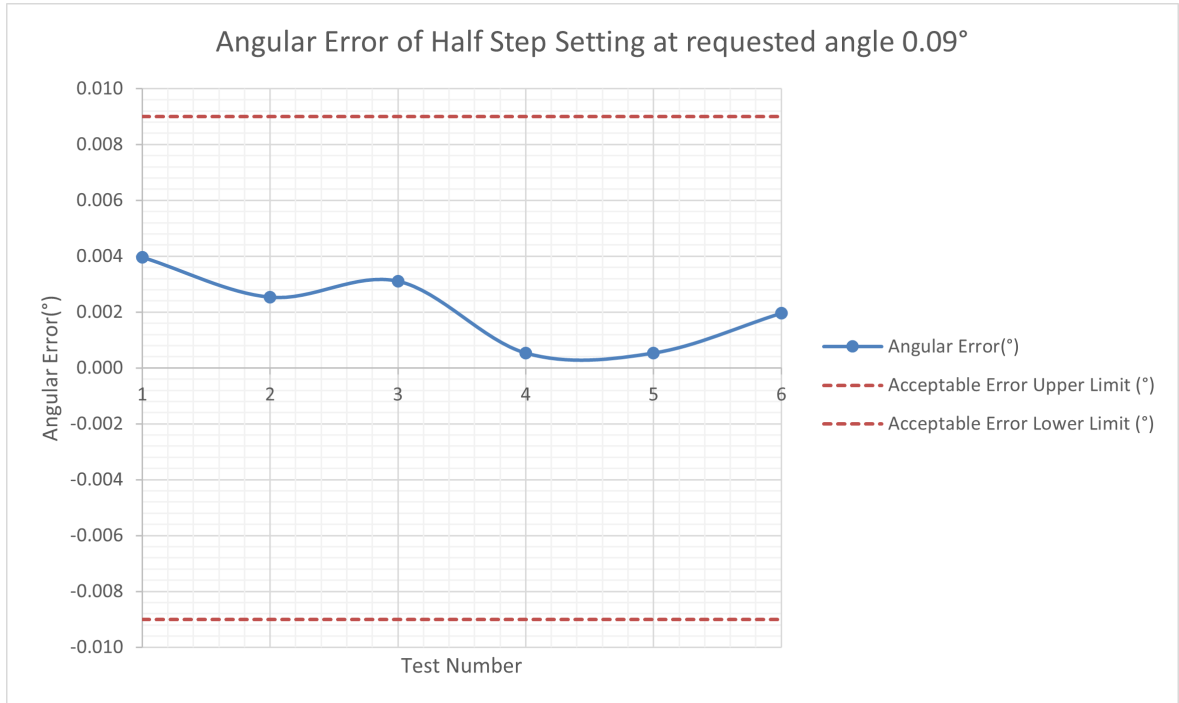


Figure 5.4: Dynamic error for the Half Step setting, showing highly stable and consistent performance.

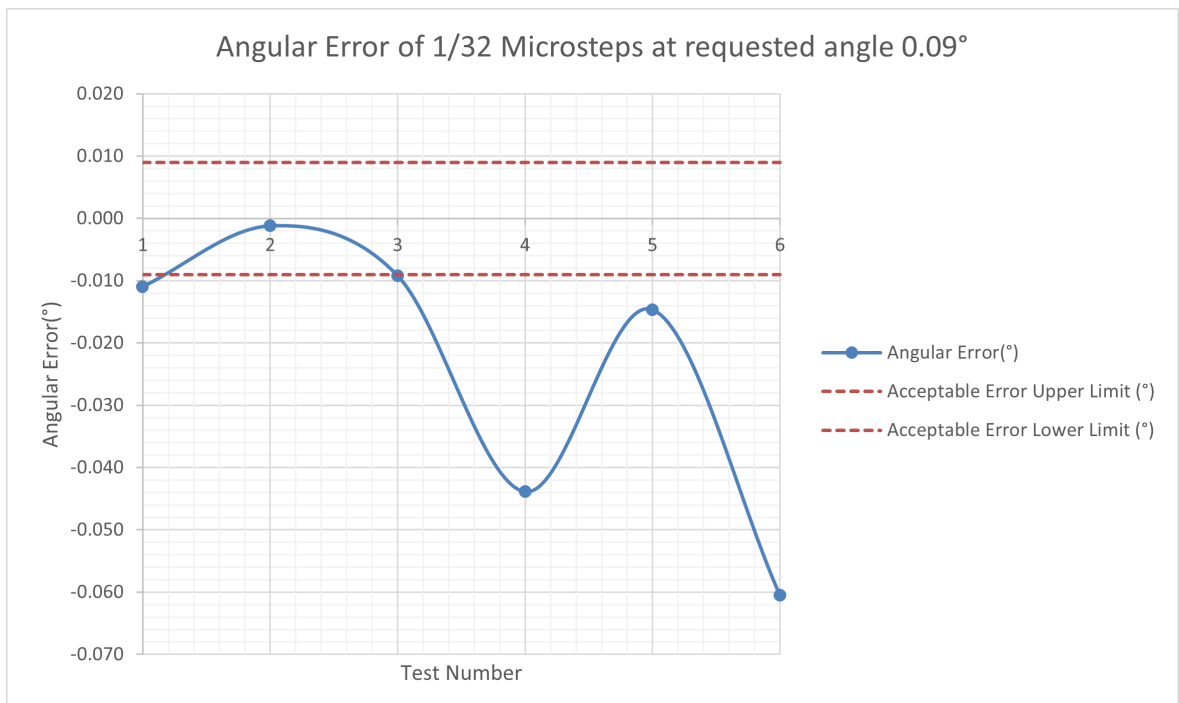


Figure 5.5: Dynamic error for the 1/32 Step setting, showing a noticeable increase in variability.

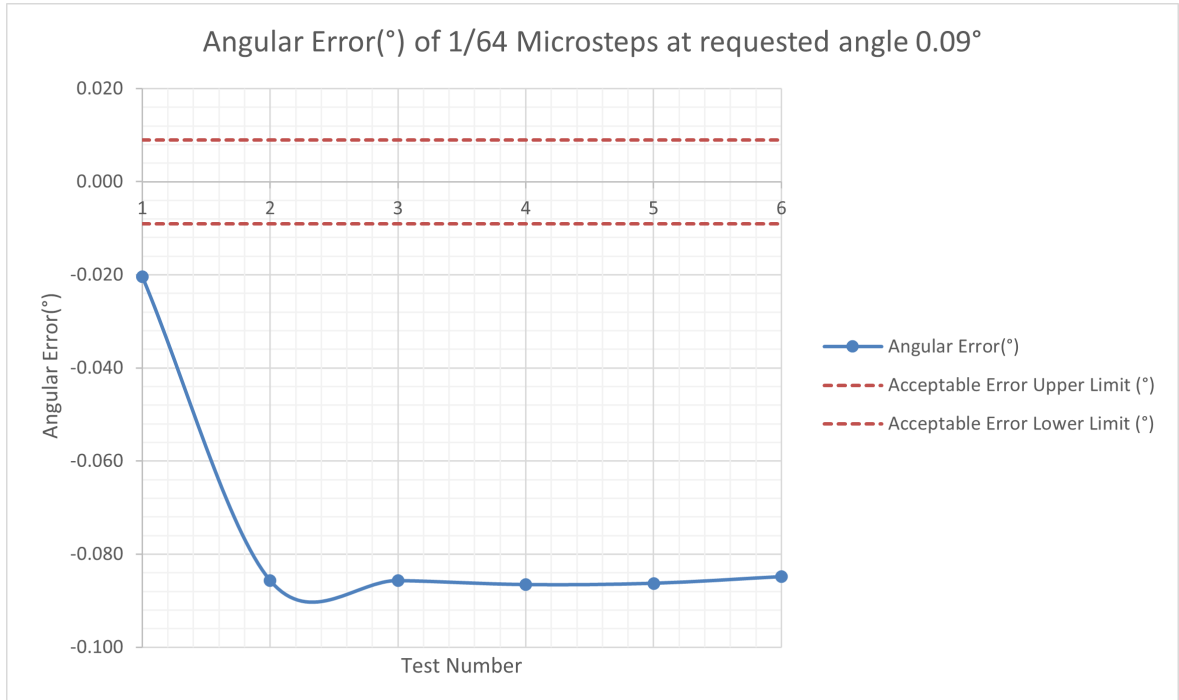


Figure 5.6: Dynamic error for the 1/64 Step setting, showing a further increase in instability.

This progressive degradation supports the conclusion that as microstepping resolution increases, the incremental torque delivered by the motor for each microstep decreases. This diminished torque is less able to consistently overcome the static friction (stiction) inherent in the cycloidal drive. The result is less uniform motion and a reduction in the effective accuracy and repeatability of the drive, despite the higher theoretical resolution presented in Table 5.2.

Finally, a note of caution should be applied when interpreting the exact magnitude of the standard deviation for the highest-resolution settings. The data sets for the 1/128 and 1/256 modes contain significantly fewer data points, which can disproportionately amplify the effect of outliers. While their poor performance is considered a genuine characteristic of the system, further testing would be required to validate the precise statistical value of their inconsistency.

# Chapter 6

## Discussion

### 6.1 Error in testing

The accuracy testing procedure had several sources of error, primarily from limitations in the measurement method and instrumentation. The setup required a human operator to mark and measure the angular displacement, introducing potential inconsistencies.

To identify angular deviation, a dry-erase marker was used to mark the laser dot projected onto a surface. However, the marker had a relatively broad tip, which made it difficult to indicate the centre of the laser point. Furthermore, the laser pointer itself introduced additional uncertainty: at a distance of 2 metres, the beam began to diverge, making it challenging to define the exact midpoint of the projection.

Measurements were taken using a set of digital callipers, which, although accurate, were susceptible to user-induced errors. These included parallax bias, where the operator's line of sight could skew the perceived alignment of the jaws, and inconsistent pressure applied during measurement. Collectively, these factors introduced uncertainty into the recorded values and reduced the reliability of the calculated angular resolution.

In future work, these limitations could be mitigated by automating the measurement process. For example, using a high-resolution camera with image processing to track laser displacement or employing a photodiode sensor array to detect beam position would yield more repeatable and accurate data. Additionally, replacing the laser pointer with a collimated beam or using a thinner marker for point registration would further improve measurement fidelity.

### 6.2 Interpolation and Control Limitations

During testing, the motor failed to actuate reliably when interpolation was enabled, so tests involving interpolated microstepping could not be completed. This was unexpected, as interpolation is typically intended to improve motion smoothness and positioning accuracy in high-resolution applications.

The issue appeared to be mechanical. Specifically, the torque generated during interpolated motion was insufficient to overcome the static friction present in the system, most notably within the cycloidal drive. Initial attempts to reduce friction involved disassembling the motor and applying a spray-on silicone lubricant to the internal components. However, this unexpectedly increased resistance, possibly due to residue thickening or surface incompatibility with the drive materials.

A second disassembly was carried out, this time replacing the spray with a generous application of silicone grease. This provided an improvement in motion smoothness and reduced some resistance, but static friction remained a significant barrier when interpolation was enabled. Ultimately, the motor was still unable to initiate movement reliably under interpolated microstepping.

This limitation prevented a full comparison between interpolated and non-interpolated performance. As such, all precision and repeatability tests documented in this report were performed with interpolation disabled. Future work may benefit from further investigation into lubrication choice, bearing preload, and potential component alignment issues, all of which may help mitigate static friction and enable functional interpolation modes.

### 6.3 Comparison of Prototype Vs Thorlabs PRM1Z8

A primary objective of this project was to develop a low-cost rotation stage that could serve as a viable alternative to expensive commercial units. The Thorlabs PRM1Z8 is a common choice for laboratory automation and serves as an excellent benchmark. The table below compares the key performance metrics of the developed prototype against the published specifications of the PRM1Z8.

Table 6.1: Performance Comparison of Prototype vs. Commercial Stage

Specification	This Project's Prototype	Thorlabs (Datasheet)[5]	PRM1Z8
Drive Mechanism	3D-Printed Cycloidal	Worm Gear	
Motor Control	Closed-Loop Stepper	Open-Loop Stepper (Optional Encoder)	
Minimum Movement	~0.09° (324 arcsec)	~0.03° (108 arcsec)	
Backlash	Not Quantified*	<0.02° (70 arcsec)	
Unidirectional Repeatability	~ ±0.01° at 1/4 microsteps (±36 arcsec)	~ ±0.0034° (±12.4 arcsec)	
Max Torque	1.47 Nm	0.4 Nm	
Estimated Cost	<£250	>£1500	

\* Backlash was not quantitatively measured but was observed to be minimal at the resolution of the test setup.

### 6.4 Price-to-Performance Analysis and Practical Significance

A direct comparison of the prototype against the Thorlabs PRM1Z8, detailed in Table 6.1, shows that the prototype does not match the benchmark's specifications for repeatability or minimum movement. However, evaluating the project on these metrics alone overlooks its primary objective: to assess the feasibility of a low-cost approach. A price-performance analysis reveals the true significance of the results.

The prototype was fabricated for an estimated cost under £225, a reduction of over 80% compared to the £1500+ commercial unit [5]. For this dramatic cost reduction, the prototype delivers remarkable performance. It achieves sub-degree precision and, critically, outperforms the commercial benchmark in one key area: maximum output torque, delivering over three times the capacity (1.47 Nm vs. 0.4 Nm). While this is partly due to the inherent strengths of the cycloidal design, it may also reflect a different design philosophy; commercial stages are often specified with lower torque to guarantee long-term reliability and minimise gear wear, a trade-off not prioritised in this proof-of-concept.

The practical significance of this result is substantial. It demonstrates that the performance gap between this prototype and a high-end commercial stage is not fundamental but is largely attributable to the trade-offs in manufacturing methods and component selection (e.g., FDM printing vs. machined metal, partially printed bearings vs. high-precision commercial bearings). This strongly suggests that a modest increase in the project budget, for instance, to incorporate a machined housing or higher grade bearings, could significantly close the gap in repeatability and backlash, while resulting in a device that is a fraction of the cost of existing commercial solutions.

### 6.5 Partially Printed Bearings

In this design, a partially printed bearing was used for the main output stage support. This approach was chosen because the primary loads are compressive and rotational speeds are low, conditions under which 3D-printed races with standard steel balls can perform adequately. This method significantly contributed to the project's low-cost goal by eliminating the need for commercially sold bearings, while also helping to save space by integrating the bearing races directly into the stage's housing design.

## 6.6 Constraints of Additive Manufacturing

While FDM printing enabled the rapid fabrication of the stage, it imposed several constraints. The primary limitation is the manufacturing tolerance. Achieving submillimeter clearances for a smooth-running cycloidal drive is challenging; layer lines and material inconsistencies can lead to friction or unwanted play.

The second constraint is the material's properties. Although PETG is robust, it cannot match the stiffness and hardness of the machined metals used in commercial stages. This may lead to minor deflections under load and limit the long-term wear resistance of the drive, potentially affecting precision over its lifetime.

## 6.7 Further Testing

### 6.7.1 Observing Wear

Post-testing analysis involved a complete disassembly of the prototype, which revealed a key design flaw. Significant wear marks were identified on the surface of the output disk, precisely corresponding to the locations of the four threaded inserts used to secure the outer housing. This indicates that the inserts made unintended contact with the disk during operation.

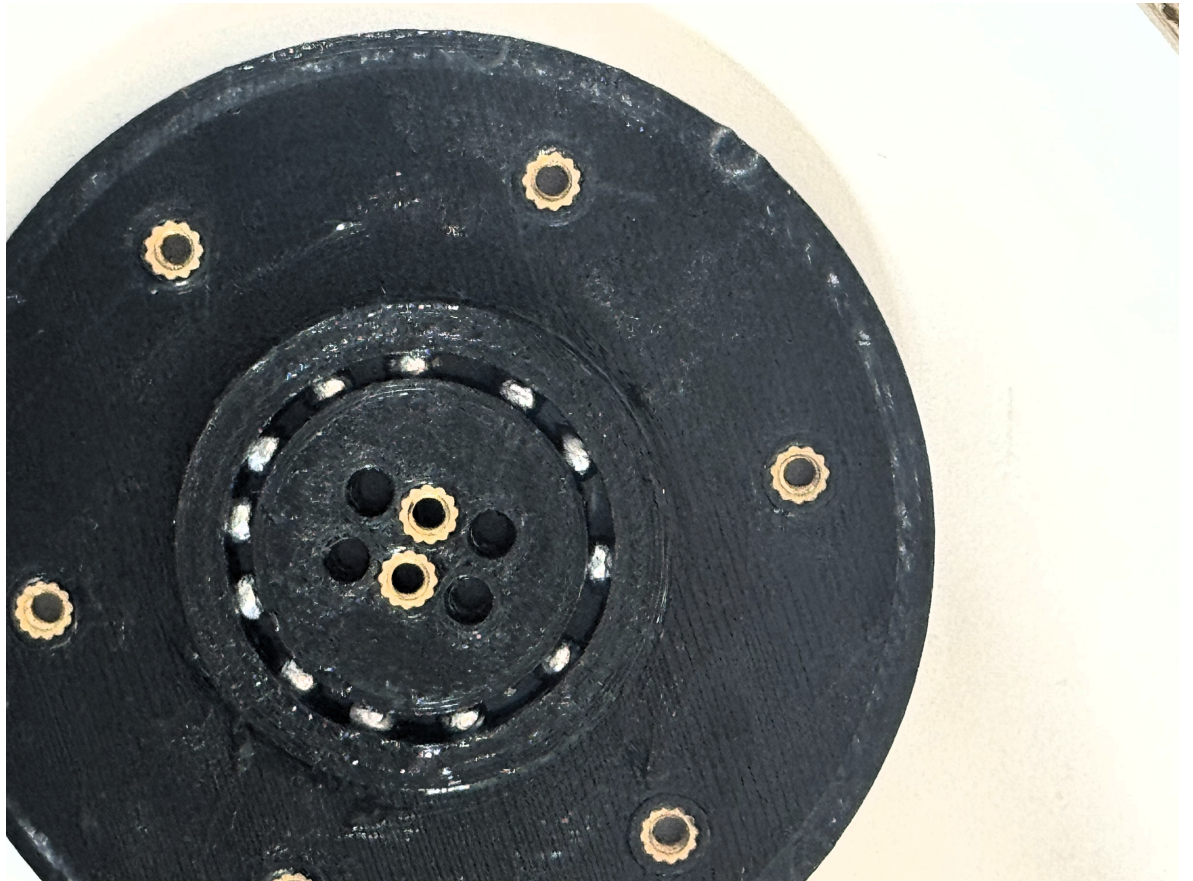


Figure 6.1: Wear marks observed on the bottom face of the output disk after disassembly, indicating unintended contact with the housing during operation.

This contact is a source of unmodeled friction, likely contributing to the control limitations observed during testing. The issue was attributed to insufficient clearance in the housing's CAD model. A future design iteration can resolve this by increasing the depth of the insert pockets by 1-2 mm, ensuring no contact occurs during rotation.

# Chapter 7

# Evaluation and Conclusion

## 7.1 Project Evaluation

This section evaluates the project, covering the methodological effectiveness and the key design trade-offs that influenced the outcome.

### 7.1.1 Effectiveness of the Hybrid Methodological Framework

The project was managed using a hybrid methodology, combining a sequential Stage-Gate model for planning with an iterative cycle for prototyping. This approach was highly effective. The initial structured phases ensured the project was built on a solid foundation of research and design, preventing costly fabrication errors. The shift to an iterative methodology during prototyping was essential for resolving the practical, unforeseen challenges of hardware development, such as tuning component clearances to minimise friction and redesigning the housing to improve mechanical stability. This blended model provided the necessary balance of formal project governance and flexibility required for a successful research and development project.

### 7.1.2 Evaluation of Project Planning: The Gantt Chart

An initial Gantt chart (see Appendix 8.4) was developed during the planning stage to provide a high-level schedule and define the key deliverables for each phase of the Stage-Gate model. This tool was effective for outlining the project's structure, including the literature review, component selection, and initial design phases.

However, as the project transitioned into the hands-on prototyping and troubleshooting stages (Stages 3 and 4), the limitations of a rigid, linear plan became apparent. The process of iterating on the hardware design, calibrating the control software, and resolving unforeseen mechanical issues required a more flexible approach than the Gantt chart could accommodate. This deviation from the initial schedule is not viewed as a failure of planning but rather as a successful application of the chosen **Hybrid Methodology**.

Ultimately, the Gantt chart served its purpose as a crucial baseline, but the project's success was dependent on the adaptability afforded by the **iterative design cycle**. This experience underscores the value of using a hybrid management approach for R&D projects that involve both predictable planning and empirical discovery.

### 7.1.3 Evaluation of Design Trade-offs

Upon reflection, the design philosophy for the prototype involved a deliberate trade-off. Rather than strictly replicating the specifications of the commercial benchmark, a key objective was to significantly increase the output torque. This decision was made with future applications in mind, where higher torque would enable the stage to handle larger and heavier resin vats, thus facilitating research into scaled-up Computed Axial Lithography.

However, this focus on maximising torque led to the implementation of a relatively high gear ratio (17:1). A direct consequence of this choice was an increase in the system's internal static friction. As observed during testing, the torque required to overcome this stiction (static friction) was greater than the incremental torque provided by the motor at its finest microstepping settings.

This effectively prevented the system from leveraging its highest theoretical resolution, creating a clear trade-off where the pursuit of higher torque for scalability compromised the achievable level of precision. This highlights a fundamental choice for future users of this design: optimising for high torque to support larger loads, or optimising for lower friction to achieve the highest possible precision.

## 7.2 Wider Context and Impact

This project was developed within the framework of **Open Science**, specifically adhering to the principles of **Free and Open-Source Hardware (FOSH)** [4, 47]. This philosophy is built on the principle that knowledge, designs, and tools should be transparent and shared freely, not only to reduce costs but also to accelerate innovation through collective action. By making the entire design process public, FOSH invites a global community to contribute improvements, identify flaws, and adapt the technology for new purposes, creating a more dynamic and robust development cycle than is possible with closed-source, proprietary products [48].

The most significant impact of this open approach is the **democratisation of scientific hardware**. The prohibitive cost of commercial equipment, which can exceed £1,500 [5], creates a major barrier for researchers. By validating a design that costs less than £225 an 85% cost reduction this project provides a tangible pathway for universities and community laboratories to acquire advanced equipment. This aligns with extensive research showing that open-source hardware provides dramatic cost savings, often between 90-99%, compared to functionally equivalent proprietary instruments [49].

This is particularly valuable for institutions in **developing countries**, where such savings are not just a convenience but a necessity. Furthermore, it empowers local scientists and engineers to build and maintain their own instruments, fostering essential technical skills and reducing long-term dependency on international supply chains for equipment and repairs. It allows for the hardware to be adapted to solve local problems, creating a more resilient and self-sufficient scientific ecosystem and directly contributing to **Equality, Diversity, and Inclusion (EDI)** in research [6].

The FOSH model also promotes **environmental sustainability** and user empowerment. Unlike commercial "black-box" systems, this open-source design embraces the "right to repair"; a user can simply 3D-print a replacement for a broken part, reducing e-waste and extending the equipment's lifespan [50]. This model of decentralised manufacturing, making parts where they are needed, also significantly reduces the carbon footprint associated with global shipping and complex logistics.

This entire framework is secured by a permissive **open-source license** (such as MIT or CERN-OHL-S). This legal tool is the critical component that guarantees the right to share ideas. It legally ensures that anyone, anywhere, can access, study, modify, and even commercialise the design, provided they adhere to the terms of the license, which have been specifically crafted to govern shared hardware designs [51]. This fosters a collaborative and sustainable ecosystem where improvements benefit everyone.

## 7.3 Lessons Learned

This project provided several key learning opportunities that extend beyond the technical results, offering valuable insights into the process of developing low-cost mechatronic hardware.

- **Theory vs. Practicality:** The most significant lesson was the divergence between theoretical performance and practical reality, especially in high-ratio gear systems. The experimental data clearly showed that the highest theoretical microstepping resolutions were not only unachievable but were detrimental to performance due to the motor's inability to overcome the drive's static friction. This highlights a critical principle: in mechatronics, system-level characteristics like friction can be a more dominant factor than the ideal specifications of any single component.
- **The Importance of Iterative Prototyping:** The project's success was heavily dependent on the iterative design cycle. Initial designs, while theoretically sound, revealed unforeseen issues during physical assembly and testing, such as the wear caused by the housing inserts. The ability to rapidly fabricate, test, identify flaws, and refine the design was essential and validated the choice of a Hybrid Methodology over a more rigid, linear approach.
- **FDM Printing as a Viable, but Constrained Tool:** Fused Deposition Modelling (FDM) proved to be an invaluable tool for creating complex, functional mechanical parts like the cycloidal drive at a very low cost. However, it also underscored the limitations of the technology regarding manufacturing tolerances. Achieving the sub-millimetre precision required for a smooth-running gearbox was a significant challenge and was the source of many of the mechanical issues that had to be overcome through iterative design.
- **The Value of Integrated Components:** The selection of an integrated closed-loop motor (the MKS SERVO42D) was a key enabling decision. While a system could be built from discrete components (a separate motor, driver, and encoder), the integrated solution significantly simplified the electronics and offloaded the complex, real-time control logic from the host microcontroller, allowing development efforts to focus on higher-level software and mechanical design.

## 7.4 Future Work and Recommended Improvements

Based on observations during testing and disassembly, several improvements for future iterations were identified.

- **Design Modifications:** To improve alignment and load capacity, duplex bearings should be incorporated into the main housing. The visibility of the cycloidal disk's alignment hole should also be improved to simplify assembly. Finally, the clearance on the bottom surface of the outer casing must be increased by at least 1 mm to prevent contact from the threaded inserts, resolving the wear issue identified in the discussion.
- **Further Testing:** A more rigorous, long-term testing regime is required for full validation. This should include endurance testing to assess wear on the 3D-printed components, quantitative backlash measurement using a dial indicator, and integration into a functional CAL system to assess its impact on final print quality.
- **Optimisation of Gearing:** Investigate alternative cycloidal gear ratios. A lower ratio would reduce internal friction and could unlock higher precision at fine microstepping settings, allowing for a study to determine the optimal balance ("sweet spot") between output torque and positioning accuracy.

## 7.5 Conclusion

This project met its primary objective: to design, fabricate, and validate a low-cost, high-torque rotation stage as a viable alternative to expensive commercial systems. The final prototype, based on a 3D-printed cycloidal drive and a closed-loop stepper motor, demonstrates a compelling price-to-performance ratio and serves as a successful proof-of-concept.

The key performance characteristics of the stage were quantified. The prototype achieved a maximum output torque of **1.47 Nm**, more than three times that of the commercial benchmark, and a practical unidirectional repeatability of **0.024°** in its optimal quarter-step mode. A critical finding was the clear trade-off between theoretical resolution and practical stability; experimental results showed that the finest microstepping settings degraded performance due to the motor's inability to overcome the drive's internal friction.

The project validates its core hypothesis. For a cost of under £250, it is feasible to create a rotation stage with performance characteristics suitable for a wide range of research applications, including Computed Axial Lithography, automated 3D scanning, and general optical experiments.

# References

- [1] Gabriel Pierce. "A feasibility study on the adaptation of a consumer-grade DLP projector for computed axial lithography". Unpublished bachelor's thesis, NMITE. 2024.
- [2] D. K. Fisher and P. J. Gould. "Open-Source Hardware Is a Low-Cost Alternative for Scientific Instrumentation and Research". In: *Modern Instrumentation* 1.2 (2012), pp. 8–20.
- [3] T. Wenzel et al. "Open hardware: From DIY trend to global transformation in access to laboratory equipment". In: *PLoS Biology* 20.1 (2022), e3001509.
- [4] Joshua M. Pearce. *Open-Source Lab: How to Build Your Own Hardware and Reduce Research Costs*. Elsevier, 2014.
- [5] Thorlabs Inc. *KPRM1Z8 - Ø1" Motorized Rotation Mount, Stepper Motor, M6 Taps*. <https://www.thorlabs.com/thorproduct.cfm?partnumber=KPRM1Z8>. Accessed June 5, 2025. Specifications for KPRM1Z8 model. 2024.
- [6] A. Maia Chagas et al. "Leveraging open hardware to alleviate the burden of COVID-19 on global health systems". In: *PLoS Biology* 18.4 (2020), e3000730.
- [7] Computed Axial Lithography Community. *OpenCAL*. GitHub Repository. Accessed: 2025-07-03. 2020. URL: <https://github.com/computed-axial-lithography/OpenCAL>.
- [8] Brian E. Kelly et al. "Volumetric Additive Manufacturing of Silica Glass with Microscale Computed Axial Lithography". In: *Advanced Materials* 33.49 (2021). Accessed June 5, 2025, p. 2104069. DOI: 10.1002/adma.202104069. URL: <https://onlinelibrary.wiley.com/doi/full/10.1002/adma.202104069>.
- [9] Robert M. Panas et al. "Micro-optics Fabrication using Blurred Tomography". In: *arXiv preprint arXiv:2401.08799* (2024). Accessed June 5, 2025. URL: <https://arxiv.org/abs/2401.08799>.
- [10] Joseph P. Toombs. "Advancements in Computed Axial Lithography: Expanding accessible materials and system capabilities". Accessed June 5, 2025. PhD thesis. University of California, Berkeley, 2022. URL: <https://escholarship.org/uc/item/4587p71q>.
- [11] Newport Corporation. *Motion Basics Terminology Standards*. <https://www.newport.com/n/motion-basics-terminology-and-standards>. Accessed June 30, 2025. 2025.
- [12] Physik Instrumente (PI) GmbH & Co. KG. *M-060, M-061, M-062 Miniature Precision Rotation Stages*. <https://www.physikinstrumente.com/en/products/rotation-stages/minature-rotation-stages/m-060-m-061-m-062-precision-rotation-stage-100260>. Accessed July 1, 2025. 2024.
- [13] HackerFab Community. *Lithography Stepper V2 Build (Work In Progress)*. <https://docs.hackerfab.org/home/fab-toolkit/patterning/lithography-stepper-v2-build-work-in-progress>. Accessed June 5, 2025. 2023.
- [14] gelstronic. *Build a 3D Printed Rotational Platform*. <https://www.instructables.com/Build-a-3D-Printed-Rotational-Platform/>. Accessed June 5, 2025. 2019.
- [15] Jonathon W. Sensinger. "Unified Approach to Cycloid Drive Profile, Stress, and Efficiency Optimization". In: *Journal of Mechanical Design* 132.2 (2010), p. 024503. DOI: 10.1115/1.4000832.
- [16] Sandeep V. Thube and Todd R. Bobak. *Dynamic Analysis of a Cycloidal Gearbox Using Finite Element Method*. Tech. rep. 12FTM17. Alexandria, VA: American Gear Manufacturers Association, 2012.
- [17] Jonathon W. Sensinger. "Efficiency of High-Sensitivity Gear Trains, Such as Cycloid Drives". In: *Journal of Mechanical Design* 135.7 (2013), p. 071006. DOI: 10.1115/1.4024370.
- [18] Joong-Ho Shin and Soon-Man Kwon. "On the lobe profile design in a cycloid reducer using instant velocity center". In: *Mechanism and Machine Theory* 41.5 (2006), pp. 596–616. DOI: 10.1016/j.mechmachtheory.2005.08.001.

- [19] Jonathon W. Sensinger and James H. Lipsey. "Cycloid vs. Harmonic Drives for use in High Ratio, Single Stage Robotic Transmissions". In: *2012 IEEE International Conference on Robotics and Automation*. Saint Paul, MN, USA, 2012, pp. 4130–4135. DOI: 10.1109/ICRA.2012.6225255.
- [20] John J. Craig. *Introduction to Robotics: Mechanics and Control*. 3rd. Upper Saddle River, NJ: Pearson/Prentice Hall, 2005. ISBN: 978-0201543612.
- [21] Daniel P. G. Nilsson, Tobias Dahlberg, and Magnus Andersson. "Step-by-step guide to 3D print motorized rotation mounts for optical applications". In: *Applied Optics* 60.13 (2021), pp. 3764–3771. DOI: 10.1364/AO.422695.
- [22] International Organization for Standardization. *ISO 492:2014 Rolling bearings — Radial bearings — Tolerances*. Standard. ISO, 2014.
- [23] Positive Altitude. *Best 3D Printed Bearing Design*. 2022. URL: [https://youtu.be/NIIYZcgJWPs?si=EBDFDrB\\_9uj47w](https://youtu.be/NIIYZcgJWPs?si=EBDFDrB_9uj47w) (visited on 06/10/2025).
- [24] Rolf Isermann. *Mechatronic Systems: Fundamentals*. London: Springer-Verlag, 2005. ISBN: 978-1852339702.
- [25] TRINAMIC Motion Control GmbH & Co. KG. *TMC2209-LA / TMC2209-SA Datasheet*. Accessed June 23, 2025. Analog Devices, Inc. May 2021. URL: [https://www.analog.com/media/en/technical-documentation/data-sheets/tmc2209\\_datasheet\\_rev1.09.pdf](https://www.analog.com/media/en/technical-documentation/data-sheets/tmc2209_datasheet_rev1.09.pdf).
- [26] DFE - Mark Andy Print Products. *Open-Loop vs. Closed-Loop Control*. <https://dfe.com/support-resources/open-loop-vs-closed-loop-control/>. Accessed July 1, 2025. 2024.
- [27] R. Krishnan. *Electric Motor Drives: Modeling, Analysis, and Control*. Upper Saddle River, NJ: Prentice Hall, 2001. ISBN: 978-0130910141.
- [28] Temesgen Lakew, Gessesse Tadesse, and Rosa Perez. "Design and Implementation of Closed-loop Stepper Motor Position Control". In: *2021 IEEE International IOT, Electronics and Mechatronics Conference (IEMTRONICS)*. 2021, pp. 1–6. DOI: 10.1109/IEMTRONICS52119.2021.9422534.
- [29] E. Galvan et al. *Motion Control Systems*. IntechOpen, 2011. ISBN: 978-953-307-527-0. DOI: 10.5772/1781.
- [30] Makerbase. *MKS SERVO42 & 57D CAN User Manual*. Version 1.0.4. Accessed June 18, 2025. Makerbase. 2023. URL: [https://github.com/makerbase-motor/MKS-SERV057D/blob/master/User%20Manual/MKS%20SERVO42%2657D\\_CAN%20User%20Manual%20V1.0.4.pdf](https://github.com/makerbase-motor/MKS-SERV057D/blob/master/User%20Manual/MKS%20SERVO42%2657D_CAN%20User%20Manual%20V1.0.4.pdf).
- [31] Bimal K. Bose. *Modern Power Electronics and AC Drives*. Upper Saddle River, NJ: Prentice Hall, 2002. ISBN: 978-0130167439.
- [32] Karl J. Åström and Tore Hägglund. *Advanced PID Control*. Research Triangle Park, NC: The Instrumentation, Systems, and Automation Society (ISA), 2006. ISBN: 978-1556179426.
- [33] Kien Minh Le, Hung Van Hoang, and Jae-Wook Jeon. "An Advanced Closed-Loop Control to Improve the Performance of Hybrid Stepper Motors". In: *IEEE Transactions on Power Electronics* 32.9 (2017), pp. 7244–7253. DOI: 10.1109/TPEL.2016.2623630.
- [34] Clarence W. de Silva. *Mechatronics: An Integrated Approach*. Describes hysteresis in actuators and mechanical systems. CRC Press, 2007, pp. 312–314.
- [35] Alexander H. Slocum. *Precision Machine Design*. Dearborn, MI: Society of Manufacturing Engineers, 1992. ISBN: 978-0872634105.
- [36] Felipe R. Maia et al. "PocketPlate: A Low-Cost and Open-Source Microplate Reader". In: *Analytical Chemistry* 94.25 (2022), pp. 8853–8858. DOI: 10.1021/acs.analchem.2c00959.

- [37] J. P. Sharkey et al. "A one-piece 3D-printed flexure translation stage for open-source microscopy". In: *Review of Scientific Instruments* 87.2 (2016), p. 025104. DOI: 10.1063/1.4941065. URL: <https://doi.org/10.1063/1.4941065>.
- [38] Joshua M. Pearce. "Open Source Hardware for Scientific Instrumentation: An Overview". In: *Instruments* 2.1 (2017), p. 2. DOI: 10.3390/instruments2010002.
- [39] HowToMechatronics. *3D Printed Gearbox - Cycloidal vs Planetary Direct Comparison*. <https://www.hwtomechatronics.com/projects/3d-printed-gearbox-cycloidal-vs-planetary/>. Accessed June 5, 2020.
- [40] stepbystep-robotics. *How to Design a Cycloidal Drive for Robot Actuator Module!* 2020. URL: <https://www.youtube.com/watch?v=Nk3aaVcvbpA&feature=youtu.be> (visited on 06/10/2025).
- [41] Robert G. Cooper. *Winning at New Products: Accelerating the Process from Idea to Launch*. 3rd. New York: Basic Books, 2001. ISBN: 978-0738204634.
- [42] Christian Johansson. "MANAGING UNCERTAINTY AND AMBIGUITY IN GATES: DECISION MAKING IN AEROSPACE PRODUCT DEVELOPMENT". In: *International Journal of Innovation and Technology Management* 11 (Dec. 2013). DOI: 10.1142/S0219877014500126.
- [43] John D. Gould and Clayton Lewis. *Designing for Usability: Key Principles and What Designers Think*. Vol. 28. 3. 1985, pp. 300–311. DOI: 10.1145/3166.3170.
- [44] Jithin Johny. *Iterative Design Process*. <https://medium.com/@jithinjohny/iterative-design-process-11d5051af3d>. Accessed July 3, 2025. Nov. 2021.
- [45] Josiah Guthrie. *PETG vs PLA Filament: Properties, Printing Examples*. <https://all3dp.com/2/petg-vs-pla-3d-printing-filaments-compared/>. Accessed July 1, 2025. June 2024.
- [46] Tian-ran Wang, Jing-shan Zhao, Shi-min Wang, et al. "An overview of the cycloidal drive: development, applications, and future trends". In: *Alexandria Engineering Journal* 95 (2024), pp. 33–51. DOI: 10.1016/j.aej.2024.05.080.
- [47] UNESCO. *UNESCO Recommendation on Open Science*. <https://unesdoc.unesco.org/ark:/48223/pf0000379949>. Accessed July 4, 2025. Paris, 2021.
- [48] Open Source Hardware Association (OSHWA). *Definition of Open Source Hardware*. <https://www.oshwa.org/definition/>. Accessed July 4, 2025. 2012.
- [49] Joshua M. Pearce. "Building Research Equipment with Free, Open-Source Hardware". In: *Science* 337.6100 (2012), pp. 1303–1304. DOI: 10.1126/science.1228183.
- [50] The European Parliament. *A longer lifetime for products: benefits for consumers and companies*. <https://www.europarl.europa.eu/news/en/headlines/society/20170505ST073551/right-to-repair-means-want-more-sustainable-and-durable-products>. Accessed July 4, 2025. 2018.
- [51] Andrew Katz. "Towards a Functional Licence for Open Hardware". In: *International Free and Open Source Software Law Review* 4.1 (2012), pp. 3–23. DOI: 10.5033/ifosslr.v4i1.62.

# Chapter 8

## Appendices

### 8.1 Project Files and Documentation

In line with the principles of Free and Open-Source Hardware (FOSH), all design files, source code, and documentation for this project are publicly available in a central online repository. This ensures that the work is fully reproducible, accessible, and open to modification by the community.

The repository contains:

- **3D Models:** All STL files required to print the components of the rotation stage.
- **Bill of materials:** A list of all 3D-printed and purchased components.
- **Control Software:** The complete, commented Python source code for the GUI control panel.
- **Electronics:** Wiring diagrams and component lists for the electronic assembly.
- **Assembly Guide:** Step-by-step instructions for assembling the mechanical and electronic components.

The project repository can be accessed at the following URL:

<https://github.com/Gacp45/Low-cost-Precision-rotation-Stage-for-CAL-Project>

Alternatively, the repository can be accessed by scanning the QR code below with a mobile device.



## 8.2 CAD Equations

```
I= 17:1
R=50mm
E=2.5mm
Rr=3.5
N=18

X = (R*cos(t))-(Rr*cos(t+arctan(sin((1-N)*t)/((R/EN)-cos((1-N)*t)))))-(E*cos(N*t))
Y = (-R*sin(t))+(Rr*sin(t+arctan(sin((1-N)*t)/((R/EN)-cos((1-N)*t)))))+(E*sin(N*t))

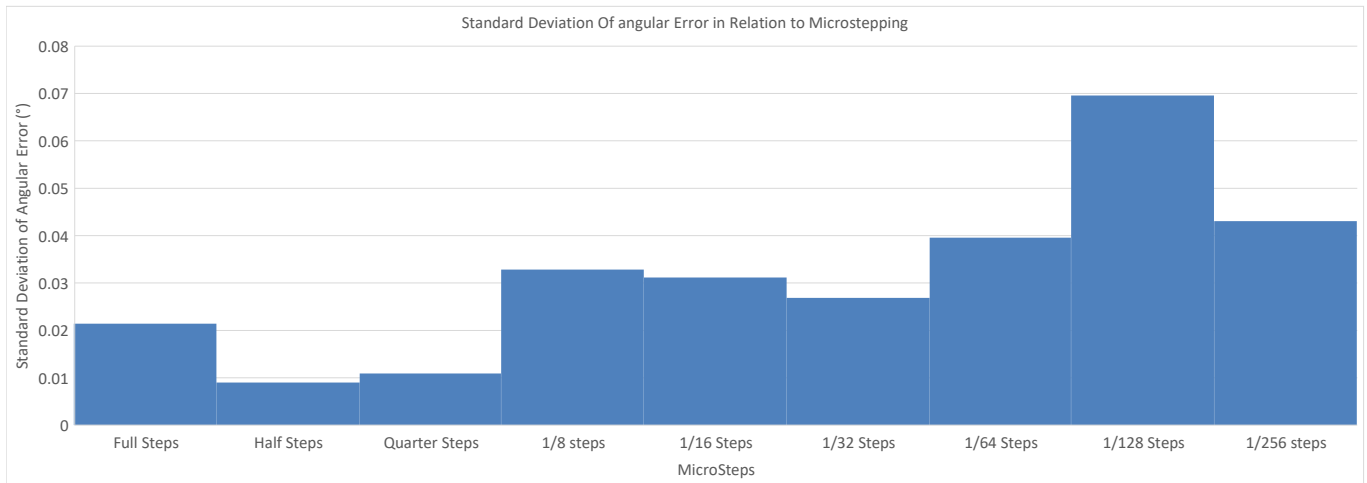
X = (50*cos(t))-(3.5*cos(t+arctan(sin((1-18)*t)/((50/2.5*18)-cos((1-18)*t)))))-(2.5*cos(18*t))
Y = (-50*sin(t))+(3.5*sin(t+arctan(sin((1-18)*t)/((50/2.5*18)-cos((1-18)*t)))))+(2.5*sin(18*t))

E < R/N
```

Figure 8.1: Parametric Equation Driven Curve

## 8.3 Precision Data

Metric	Full Steps	Half Steps	Quarter Steps	1/8 steps	1/16 Steps	1/32 Steps	1/64 Steps	1/128 Steps	1/256 steps
Average Error	0.0063	-0.0056	-0.0094	-0.0137	-0.0135	-0.0093	-0.0253	-0.0323	-0.0306
Max Error	0.0644	0.004	0.0019	0.0435	0.0437	0.0492	0.0194	0.0655	0.016
Standard Deviation	0.021476673	0.00903699	0.010975537	0.032904479	0.031210579	0.026932405	0.039607204	0.069629954	0.043094114
Lower 2sigma limit	-0.036653345	-0.02367398	-0.031351074	-0.079508958	-0.075921158	-0.063164811	-0.104514407	-0.171559908	-0.116788227
Upper 2sigma limit	0.049253345	0.01247398	0.012551074	0.052108958	0.048921158	0.044564811	0.053914407	0.106959908	0.055588227



Summary

Test #	Commanded Angle (°)	Distance to Wall (mm)	Expected Displacement (mm)	Measured Displacement (mm)	Absolute Error (mm)	Error (%)	Average Error %	Notes
1	0.38	2000	13.26	15.51	2.25	16.93		full step interp on, Only works with SR_FOC
2	0.38	2000	13.26	12.7	0.56	4.26		
3	0.38	2000	13.26	13.04	0.22	1.69		
4	0.38	2000	13.26	13.26	0.42	3.00		
5	0.38	2000	13.26	13.24	0.02	0.19		
6	0.38	2000	13.26	12.76	0.50	3.80	5.01	
1	0.38	2000	13.26	10.85	2.41	18.20		Half step interp on
2	0.38	2000	13.26	10.91	2.35	17.75		
3	0.38	2000	13.26	11.2	2.06	15.57		
4	0.38	2000	13.26	11.01	2.25	17.00		
5	0.38	2000	13.26	10.16	3.10	23.41		
6	0.38	2000	13.26	11.07	2.19	16.55	18.08	
1	0.38	2000	13.26	11.08	2.18	16.47		quarter step interp on
2	0.38	2000	13.26	11.1	1.66	12.55		
3	0.38	2000	13.26	11.97	1.29	9.76		
4	0.38	2000	13.26	12.05	1.21	9.16		
5	0.38	2000	13.26	13.71	0.45	3.36		
6	0.38	2000	13.26	12.7	0.56	4.26	9.26	
1	0.38	2000	13.26	12.23	1.03	7.80		1/8 Step
2	0.38	2000	13.26	10.75	2.51	18.96		
3	0.38	2000	13.26	12.18	1.08	8.18		
4	0.38	2000	13.26	13.26	0.00	0.04		
5	0.38	2000	13.26	11.3	1.96	14.81		
6	0.38	2000	13.26	11.52	1.71	12.93	10.45	
1	0.38	2000	13.26	12.05	1.00	9.08		1/16th
2	0.38	2000	13.26	12.14	1.12	8.48		
3	0.38	2000	13.26	12.13	1.13	8.55		
4	0.38	2000	13.26	10.27	2.99	22.58		
5	0.38	2000	13.26	10.51	2.75	20.77		
6	0.38	2000	13.26	12.01	1.25	9.46	13.15	
1	0.38	2000	13.26	12.16	1.10	8.33		1/32s
2	0.38	2000	13.26	11.9	1.36	10.29		
3	0.38	2000	13.26	12.69	0.57	4.33		
4	0.38	2000	13.26	8.27	4.99	37.65		
5	0.38	2000	13.26	4.39	8.87	66.90		
6	0.38	2000	13.26	10	2.61	24.51	25.35	
1	0.38	2000	13.26	15.71	2.45	18.43		1/64th
2	0.38	2000	13.26	13.38	0.12	0.87		
3	0.38	2000	13.26	13.17	0.09	0.71		
4	0.38	2000	13.26	13.24	0.02	0.19		
5	0.38	2000	13.26	13.24	0.02	0.19		
6	0.38	2000	13.26	13.29	0.03	0.19	3.43	
1	0.38	2000	13.26	13.18	0.08	0.64		1/128th
2	0.38	2000	13.26	13.1	0.16	1.24		
3	0.38	2000	13.26	15	2.96	22.35		
4	0.38	2000	13.26	12.42	0.84	6.37		
5	0.38	2000	13.26	13.36	0.10	0.72		Rezeroed
6	0.38	2000	13.26	12.48	0.78	5.92	6.21	
1	0.38	2000	13.26	11.87	1.39	10.51		1/256th
2	0.38	2000	13.26	10.99	2.27	17.15		
3	0.38	2000	13.26	13.37	0.11	0.79		
4	0.38	2000	13.26	13.64	0.38	2.83		
5	0.38	2000	13.26	11.69	1.57	11.87		
6	0.38	2000	13.26	13.31	0.05	0.34	7.25	

0.38 Interp on

Test #	Commanded Angle (°)	Distance to Wall (mm)	Expected Displacement (mm)	Measured Displacement (mm)	Absolute Error (mm)	Error (%)	Average Error %	Notes
1	0.09	2000	3.14	5.39	2.25	71.57		full steps interp off, Results have been Tested again AFTER Changing mode to SR_CLOSE
2	0.09	2000	3.14	2.33	1.00	44.44		
3	0.09	2000	3.14	2.38	0.76	24.24		
4	0.09	2000	3.14	3.39	0.25	7.91		
5	0.09	2000	3.14	3.25	0.11	3.45		
6	0.09	2000	3.14	4.44	1.30	41.33	27.99	
1	0.09	2000	3.14	3.28	0.14	4.41		
2	0.09	2000	3.14	3.23	0.09	2.81		
3	0.09	2000	3.14	3.25	0.11	3.45		
4	0.09	2000	3.14	3.16	0.02	0.59		
5	0.09	2000	3.14	3.16	0.02	0.59		
6	0.09	2000	3.14	3.21	0.07	2.18	2.34	
1	0.09	2000	3.14	1.95	1.19	75.93		4 microstep interp off, cooling laser after test
2	0.09	2000	3.14	3.07	0.07	2.28		
3	0.09	2000	3.14	2.06	1.08	34.43		
4	0.09	2000	3.14	2.51	0.63	20.10		
5	0.09	2000	3.14	2.18	0.96	30.61		
6	0.09	2000	3.14	2.87	0.27	8.65	22.33	
1	0.09	2000	3.14	2.77	0.37	11.83		8 microstep interp off
2	0.09	2000	3.14	2.93	0.12	4.14		
3	0.09	2000	3.14	3.14	0.00	0.06		
4	0.09	2000	3.14	3.08	0.06	1.96		
5	0.09	2000	3.14	3.01	0.13	4.19		
6	0.09	2000	3.14	3	0.14	4.51	4.88	
1	0.09	2000	3.14	2.84	0.30	9.60		16 microstep interp off
2	0.09	2000	3.14	3.06	0.08	2.60		
3	0.09	2000	3.14	3.08	0.06	1.96		
4	0.09	2000	3.14	2.91	0.23	7.37		
5	0.09	2000	3.14	3.11	0.03	1.01		
6	0.09	2000	3.14	2.99	0.15	4.83	4.56	
1	0.09	2000	3.14	2.76	0.38	12.15		32 microstep interp off
2	0.09	2000	3.14	3.1	0.04	1.27		
3	0.09	2000	3.14	2.32	0.32	10.24		
4	0.09	2000	3.14	1.61	1.53	48.75		
5	0.09	2000	3.14	2.63	0.51	16.28		
6	0.09	2000	3.14	1.03	2.11	67.21	25.99	
1	0.09	2000	3.14	2.43	0.71	22.65		64 microstep interp off. Must have been at a point where it could get past static friction.
2	0.09	2000	3.14	0.15	2.99	95.3		Backlash? Not enough Torque to drive Stage at this angle
3	0.09	2000	3.14	0.15	2.92	95.23		Backlash again
4	0.09	2000	3.14	0.12	3.02	95.18		Backlash again
5	0.09	2000	3.14	0.13	3.01	95.86		Backlash again
6	0.09	2000	3.14	0.18	2.96	94.27	83.24	Backlash again

0.00 interp off

Test #	Commanded Angle (°)	Distance to Wall (mm)	Expected Displacement (mm)	Measured Displacement (mm)	Absolute Error (mm)	Error (%)	Average Error	Notes
1	0.18	2000	6.28	6.09	0.19	3.074958529	5.843152684	full steps interp off
2	0.18	2000	6.28	7.18	0.90	14.2728732		
3	0.18	2000	6.28	5.94	0.34	5.462274821		Full steps interp off. 1 RPM 1 Accel
4	0.18	2000	6.28	5.89	0.39	6.258046919		Full steps interp off. 1 RPM 1 Accel
5	0.18	2000	6.28	6	0.28	4.507348304		
6	0.18	2000	6.28	6.19	0.09	1.483414334		
1	0.18	2000	6.28	6.3	0.02	0.26728428	6.214512996	1/2 steps interp off. Stage Settled quickly, Minimal Error
2	0.18	2000	6.28	6.03	0.25	4.029885046		1/2 steps interp off. Stage Settled quickly, Minimal Error
3	0.18	2000	6.28	5.25	1.03	16.44392977		Cable Plugged into Laser, Potentially affecting Accuracy due to Added friction?
4	0.18	2000	6.28	5.67	0.61	9.759444148		
5	0.18	2000	6.28	6.22	0.06	1.005951075		
6	0.18	2000	6.28	5.92	0.36	5.78058366		
1	0.18	2000	6.28	5.89	0.39	6.258046919	2.324747269	4 microstep interp on, accidental
2	0.18	2000	6.28	6.05	0.23	3.711576207		4 microstep interp on, accidental
3	0.18	2000	6.28	6.17	0.11	1.801723173		4 MS Interp on Accidental
4	0.18	2000	6.28	6.31	0.03	4.0264387		4 MS Interp on Accidental
5	0.18	2000	6.28	6.24	0.04	0.687642237		4 MS Interp on Accidental
6	0.18	2000	6.28	6.35	0.07	1.063056378		4 MS Interp on Accidental
1	0.18	2000	6.28	7.08	0.80	12.681329	10.57627826	8 microstep interp off. Anomalous result?
2	0.18	2000	6.28	6.42	0.14	2.177137314		
3	0.18	2000	6.28	7.1	0.82	12.99963784		
4	0.18	2000	6.28	7.8	1.52	24.1404472		
5	0.18	2000	6.28	6.77	0.49	7.747541997		
6	0.18	2000	6.28	6.05	0.23	3.711576207		
1	0.18	2000	6.28	6.09	0.19	3.074958529	10.54023497	16 microstep interp off
2	0.18	2000	6.28	7.33	1.05	16.66018949		
3	0.18	2000	6.28	7.81	1.53	24.29960162		
4	0.18	2000	6.28	6.89	0.61	9.657395031		
5	0.18	2000	6.28	6.13	0.15	2.438340851		
6	0.18	2000	6.28	6.73	0.45	7.110924319		
1	0.18	2000	6.28	4.59	1.69	26.94812145	15.99501916	32 microstep interp off
2	0.18	2000	6.28	8	1.72	27.3235359		zeroing is slightly off
3	0.18	2000	6.28	6.7	0.42	6.63346106		
4	0.18	2000	6.28	6	0.28	4.507348304		
5	0.18	2000	6.28	5.22	1.06	16.92139902		
6	0.18	2000	6.28	7.14	0.86	13.63625552		
1	0.18	2000	6.28	6.62	0.34	5.360225704	4.791640771	64 microstep interp off
2	0.18	2000	6.28	5.84	0.44	7.053819016		
3	0.18	2000	6.28	6.11	0.17	2.75664969		
4	0.18	2000	6.28	6.11	0.17	2.75664969		
5	0.18	2000	6.28	6.96	0.68	10.77147597		
6	0.18	2000	6.28	6.28	0.00	0.051024559		
1	0.18	2000	6.28	7.57	1.29	20.47989556	22.48633399	128 microstep, interp off
2	0.18	2000	6.28	8.57	2.29	36.39533751		128 microstep, interp off
3	0.18	2000	6.28	8.45	2.17	34.48548447		128 microstep, interp off
4	0.18	2000	6.28	6.37	0.09	1.381365217		Cable Plugged in Angle different. 128 microstep, Interp off
5	0.18	2000	6.28	5	1.28	20.42279025		Cable Plugged in Angle different. 128 microstep, Interp off
6	0.18	2000	6.28	7.65	1.37	21.75313091		Cable Plugged in Angle different. 128 microstep, Interp off
1	0.18	2000	6.28	6.84	0.56	8.861622933	5.172518634	256 microstep, interp off
2	0.18	2000	6.28	6.49	0.21	3.291218251		256 microstep, interp off
3	0.18	2000	6.28	6.1	0.18	2.915804109		256 microstep, interp off
4	0.18	2000	6.28	6.12	0.16	2.59749527		256 microstep, interp off
5	0.18	2000	6.28	6.46	0.18	2.813754992		256 microstep, interp off
6	0.18	2000	6.28	5.62	0.66	10.55521625		256 microstep, interp off

0.18 interp off

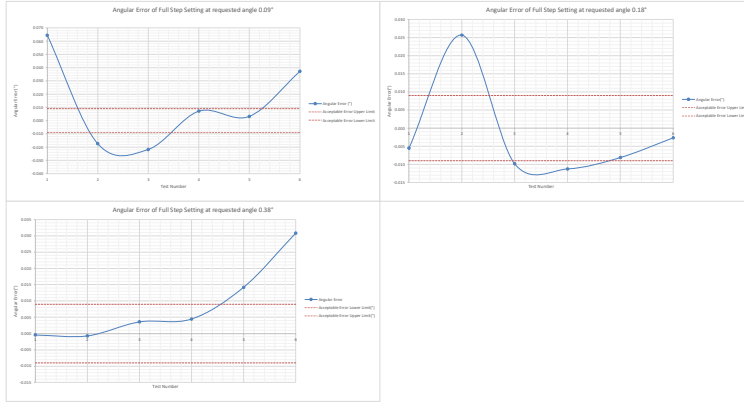
Test #	Commanded Angle (°)	Distance to Wall (mm)	Expected Displacement (mm)	Measured Displacement (mm)	Absolute Error (mm)	Error (%)	Average Error	Notes
1	0.38	2000	13.26	13.25	0.014696806	0.110796396	2.37548637	full steps interp off
2	0.38	2000	13.26	13.24	0.024696806	0.186184475		
3	0.38	2000	13.26	13.39	0.125303194	0.944636698		
4	0.38	2000	13.26	13.42	0.155303194	1.170800933		
5	0.38	2000	13.26	13.76	0.495303194	3.733995591		
6	0.38	2000	13.26	14.34	1.075303194	8.106504126		
1	0.38	2000	13.26	12.9	0.364696806	2.749379133	2.108580468	1/2 steps interp off
2	0.38	2000	13.26	12.62	0.644696806	4.860245322		
3	0.38	2000	13.26	12.97	0.294696806	2.221662586		
4	0.38	2000	13.26	13.03	0.234696806	1.769334117		
5	0.38	2000	13.26	13.16	0.104696806	0.7892891		
6	0.38	2000	13.26	13.23	0.034696806	0.261572553		
1	0.38	2000	13.26	13.2	0.064696806	0.487736787	1.241617569	4 microstep interp off
2	0.38	2000	13.26	13.12	0.144696806	1.090841413		
3	0.38	2000	13.26	13.1	0.164696806	1.241617569		
4	0.38	2000	13.26	13.18	0.084696806	0.638512944		
5	0.38	2000	13.26	13	0.264696806	1.995498351		
6	0.38	2000	13.26	13	0.264696806	1.995498351		
1	0.38	2000	13.26	12.17	1.094696806	8.252708841	14.07015554	8 microstep interp off
2	0.38	2000	13.26	11.42	1.844696806	13.90681471		
3	0.38	2000	13.26	11.31	1.954696806	14.73608357		
4	0.38	2000	13.26	10.5	2.764696806	20.8425179		
5	0.38	2000	13.26	11.31	1.954696806	14.73608357		
6	0.38	2000	13.26	11.68	1.584696806	11.94672467		
1	0.38	2000	13.26	11.54	1.724696806	13.00215777	13.73090919	16 microstep interp off
2	0.38	2000	13.26	11.54	1.724696806	13.00215777		
3	0.38	2000	13.26	11.36	1.904696806	14.35914317		
4	0.38	2000	13.26	11.34	1.924696806	14.50991933		
5	0.38	2000	13.26	11.33	1.934696806	14.58530741		
6	0.38	2000	13.26	11.55	1.714696806	12.92676969		
1	0.38	2000	13.26	11.99	1.274696806	9.069694248	2.062131285	32 microstep interp off
2	0.38	2000	13.26	13.34	0.075303194	0.567696307		
3	0.38	2000	13.26	13.33	0.065303194	0.492308229		
4	0.38	2000	13.26	13.48	0.215303194	1.623129402		
5	0.38	2000	13.26	13.27	0.005303194	0.03997976		
6	0.38	2000	13.26	13.27	0.005303194	0.03997976		
1	0.38	2000	13.26	13.52	0.255303194	1.924681715	1.255706063	64 microstep interp off
2	0.38	2000	13.26	13.21	0.054696806	0.412348709		
3	0.38	2000	13.26	13.26	0.004696806	0.035408318		
4	0.38	2000	13.26	12.98	0.284696806	2.146274508		
5	0.38	2000	13.26	13.31	0.045303194	0.341532073		
6	0.38	2000	13.26	12.91	0.354696806	2.673991055		
1	0.38	2000	13.26	11.25	2.014696806	15.18841203	24.42345161	128 microstep, interp off
2	0.38	2000	13.26	9.57	3.694696806	27.85360917		128 microstep, interp off
3	0.38	2000	13.26	9.86	3.404696806	25.6673549		128 microstep, interp off
4	0.38	2000	13.26	10.27	2.994696806	22.5764437		Cable Plugged in Angle different. 128 microstep, Interp off
5	0.38	2000	13.26	9.64	3.624696806	27.32589262		Cable Plugged in Angle different. 128 microstep, Interp off
6	0.38	2000	13.26	9.56	3.704696806	27.92899725		Cable Plugged in Angle different. 128 microstep, Interp off
1	0.38	2000	13.26	13.24	0.024696806	0.186184475	15.99255154	256 microstep, interp off
2	0.38	2000	13.26	12.28	0.984696806	7.423439981		256 microstep, interp off
3	0.38	2000	13.26	9.11	4.154696806	31.32146077		256 microstep, interp off
4	0.38	2000	13.26	10.26	3.004696806	22.65183178		256 microstep, interp off
5	0.38	2000	13.26	11.02	2.244696806	16.92233783		256 microstep, interp off
6	0.38	2000	13.26	10.95	2.314696806	17.45005438		256 microstep, interp off

0.38 interp off

Test #	Commanded Angle (°)	Actual Angle(°)	Angular Error(°)	Distance to Wall (mm)	Expected Displacement (mm)	Measured Displacement (mm)	Absolute Error (mm)	Error (%)	Notes
1	0.09	0.154	0.064	2000	3.14	5.39	2.25	71.57	full steps interp off, Results have been Tested again AFTER Changing mode to SR CLOSE
2	0.09	0.077	-0.021	2000	3.14	3.33	0.19	5.94	
3	0.09	0.068	-0.022	2000	3.14	2.38	0.76	24.24	
4	0.09	0.097	0.007	2000	3.14	3.39	0.25	7.91	
5	0.09	0.093	0.003	2000	3.14	3.25	0.11	3.45	
6	0.09	0.127	0.037	2000	3.14	4.44	1.30	41.13	
7	0.18	0.174	-0.006	2000	6.28	6.09	0.19	3.07	full steps interp off
8	0.18	0.206	0.026	2000	6.28	7.18	0.90	14.27	
9	0.18	0.170	-0.010	2000	6.28	5.84	0.14	5.47	full steps interp off, 1 RPM 1 Accel
10	0.18	0.169	-0.011	2000	6.28	5.89	0.19	6.26	full steps interp off, 1 RPM 1 Accel
11	0.18	0.172	-0.008	2000	6.28	6	0.28	4.51	
12	0.18	0.177	-0.007	2000	6.28	6.19	0.09	1.44	
13	0.18	0.180	0.000	2000	13.26	13.25	0.01	0.11	full steps interp off
14	0.18	0.179	-0.001	2000	13.26	13.24	0.02	0.19	
15	0.18	0.184	0.004	2000	13.26	13.39	0.13	0.94	
16	0.18	0.188	0.006	2000	13.26	13.42	0.16	1.17	
17	0.18	0.194	0.014	2000	13.26	13.76	0.50	3.73	
18	0.18	0.194	0.011	2000	13.26	14.34	1.08	8.11	

Average 0.52  
Max 2.25  
Min 0.01  
StDev 0.021476973

Acceptable Error  
1 0.009  
2 0.009  
3 0.009  
4 0.009  
5 0.009  
6 0.009  
1 -0.009  
2 -0.009  
3 -0.009  
4 -0.009  
5 -0.009  
6 -0.009

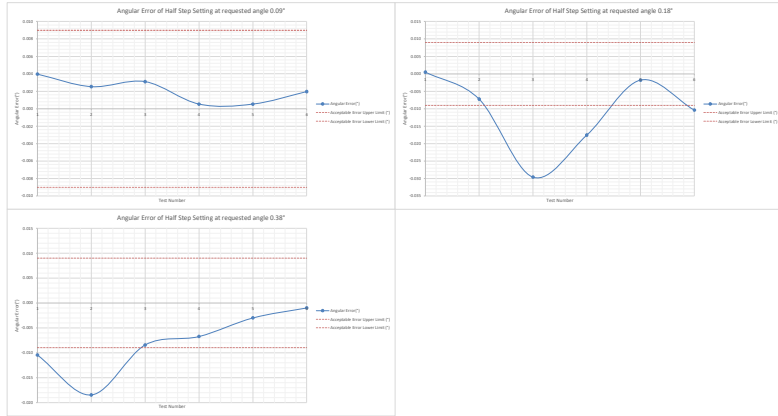


Full Steps Sheet

Test #	Commanded Angle [°]	Actual Angle [°]	Angular Error [°]	Distance to Wall (mm)	Expected Displacement (mm)	Measured Displacement (mm)	Absolute Error (mm)	Angular Positioning Error (%)	NOTES
1	0.09	0.094	0.004	2000	3.14	3.28	0.14	4.4	4.1/2 steps interp off, Mode on Encoder changed to SR_CLOSE. Realised previous testing was on wrong mode... FULLSTEPS WILL BE RETESTED
2	0.09	0.093	0.003	2000	3.14	3.23	0.09	2.8	
3	0.09	0.095	0.005	2000	3.14	3.23	0.11	3.5	
4	0.09	0.091	0.001	2000	3.14	3.16	0.02	0.6	
5	0.09	0.091	0.001	2000	3.14	3.16	0.02	0.6	
6	0.09	0.092	0.002	2000	3.14	3.21	0.07	2.2	
1	0.18	0.180	0.000	2000	6.28	6.18	0.00	0.3	1/2 steps interp off, Stage Settled quickly, Minimal Error
2	0.18	0.173	-0.007	2000	6.28	6.03	0.25	4.0	1/2 steps interp off, Stage Settled quickly, Minimal Error
3	0.18	0.150	-0.030	2000	6.28	5.25	1.03	16.4	Cable Plugged into Laser, Potentially affecting Accuracy due to Added friction?
4	0.18	0.162	-0.018	2000	6.28	5.67	0.61	9.8	
5	0.18	0.179	-0.010	2000	6.28	5.27	0.64	1.5	
6	0.18	0.170	-0.010	2000	6.28	5.92	0.36	5.8	
1	0.38	0.370	-0.010	2000	13.26	12.9	0.36	2.7	1/2 steps interp off
2	0.38	0.362	-0.018	2000	13.26	12.62	0.64	4.9	
3	0.38	0.373	-0.008	2000	13.26	13.35	0.09	2.3	
4	0.38	0.373	-0.007	2000	13.26	13.03	0.23	1.8	
5	0.38	0.377	-0.003	2000	13.26	13.16	0.10	0.8	
6	0.38	0.379	-0.001	2000	13.26	13.23	0.03	0.3	

Average 0.25  
Max 1.03  
Min 0.02  
SDev 0.0093969

Acceptable Error	Acceptable Error Upper Limit [°]	Acceptable Error Lower Limit [°]
1	0.009	-0.009
2	0.009	-0.009
3	0.009	-0.009
4	0.009	-0.009
5	0.009	-0.009
6	0.009	-0.009

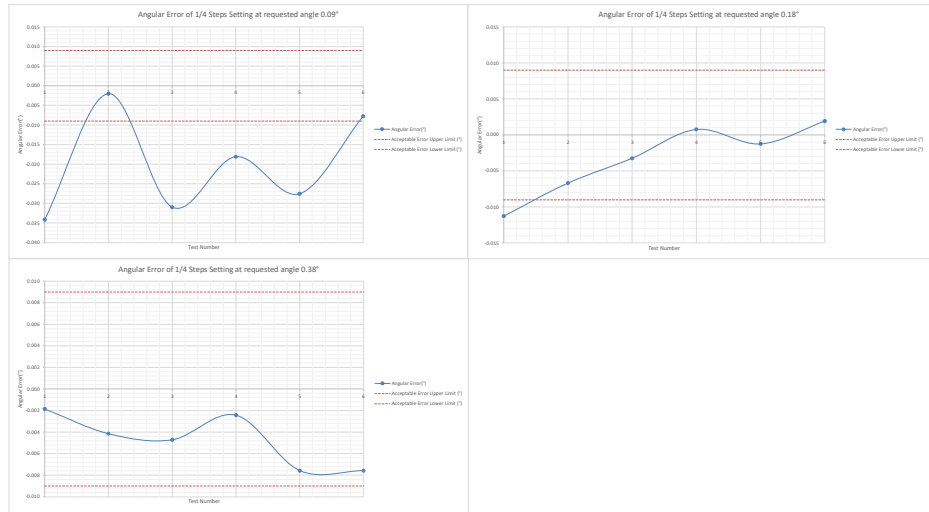


Half Steps

Test #	Commanded Angle (°)	Actual Angle (°)	Angular Error (°)	Distance to Wall (mm)	Expected Displacement (mm)	Measured Displacement (mm)	Absolute Error (mm)	Error (%)	Notes
1	0.09	0.056	-0.034	2000	3.14	1.95	1.19	37.93	4 microstep interp off, cooling laser after test
2	0.09	0.068	-0.007	2000	3.14	3.07	0.07	2.28	
3	0.09	0.059	-0.021	2000	3.14	2.22	1.03	43	
4	0.09	0.072	-0.018	2000	3.14	2.51	0.63	20.10	
5	0.09	0.062	-0.028	2000	3.14	2.18	0.96	30.61	
6	0.09	0.082	-0.008	2000	3.14	2.87	0.27	8.65	
1	0.18	0.169	-0.011	2000	6.28	5.89	0.39	6.26	4 microstep interp on, accidental
2	0.18	0.173	-0.007	2000	6.28	6.05	0.23	3.71	4 microstep interp on, accidental
3	0.18	0.177	-0.003	2000	6.28	6.17	0.11	3.71	4 microstep interp on, accidental
4	0.18	0.161	0.001	2000	6.28	6.31	0.03	0.43	4 MS Interp on Accidental
5	0.18	0.179	-0.001	2000	6.28	6.24	0.04	0.69	4 MS Interp on Accidental
6	0.18	0.182	0.002	2000	6.28	6.35	0.07	1.06	4 MS Interp on Accidental
1	0.38	0.378	-0.002	2000	13.26	13.21	0.06	0.49	4 microstep interp off
2	0.38	0.376	-0.004	2000	13.26	13.12	0.14	1.09	
3	0.38	0.375	-0.005	2000	13.26	13.1	0.16	1.24	
4	0.38	0.378	-0.002	2000	13.26	13.18	0.08	0.64	
5	0.38	0.372	-0.008	2000	13.26	13	0.26	2.00	
6	0.38	0.372	-0.008	2000	13.26	13	0.26	2.00	

Average 0.34  
Max 13.2  
Min 0.03  
StDev 0.010975537

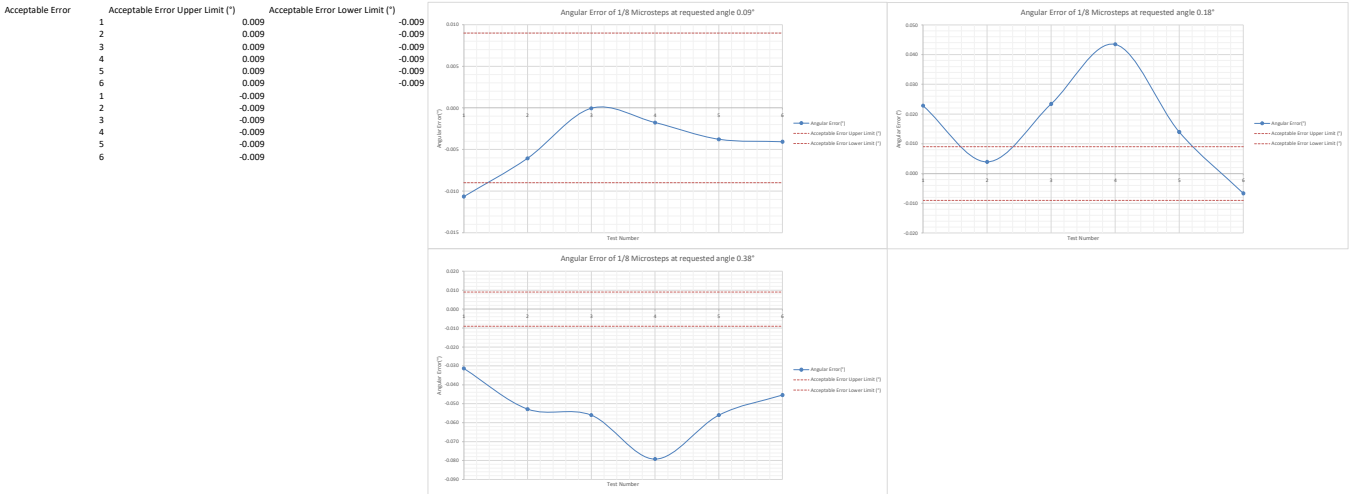
Acceptable Error	Acceptable Error Upper Limit (°)	Acceptable Error Lower Limit (°)
1	0.009	-0.009
2	0.009	-0.009
3	0.009	-0.009
4	0.009	-0.009
5	0.009	-0.009
6	0.009	-0.009
1	-0.009	
2	-0.009	
3	-0.009	
4	-0.009	
5	-0.009	
6	-0.009	



Quarter Steps

Test #	Commanded Angle (°)	Actual Angle (°)	Angular Error (°)	Distance to Wall (mm)	Expected Displacement (mm)	Measured Displacement (mm)	Absolute Error (mm)	Error (%)	Notes
1	0.09	0.079	-0.011	2000	3.14	2.77	0.37	11.83	8 microstep interp off
2	0.09	0.084	-0.006	2000	3.14	2.93	0.21	6.74	
3	0.09	0.090	0.006	2000	3.14	3.14	0.00	0.05	
4	0.09	0.086	-0.003	2000	3.14	3.08	0.06	1.96	
5	0.09	0.086	-0.004	2000	3.14	3.01	0.13	4.19	
6	0.09	0.096	-0.004	2000	3.14	3	0.14	4.53	
1	0.18	0.203	0.023	2000	6.28	7.08	0.80	12.68	8 microstep interp off. Anomalous result?
2	0.18	0.184	-0.004	2000	6.28	6.42	0.14	2.18	
3	0.18	0.203	0.023	2000	6.28	7.1	0.82	13.00	
4	0.18	0.223	0.043	2000	6.28	7.8	1.52	24.14	
5	0.18	0.19	-0.001	2000	6.28	6.77	0.99	7.75	
6	0.18	0.173	-0.007	2000	6.28	6.05	0.33	3.21	
1	0.38	0.349	-0.021	2000	13.26	12.17	1.09	8.25	8 microstep interp off
2	0.38	0.327	-0.053	2000	13.26	11.42	1.84	13.91	
3	0.38	0.324	-0.056	2000	13.26	11.31	1.95	14.74	
4	0.38	0.301	-0.079	2000	13.26	10.5	2.76	20.84	
5	0.38	0.324	-0.056	2000	13.26	11.31	1.95	14.74	
6	0.38	0.335	-0.045	2000	13.26	11.68	1.58	11.95	

Average 0.89  
Max 2.76  
Min 2.77  
StDev 0.032904479

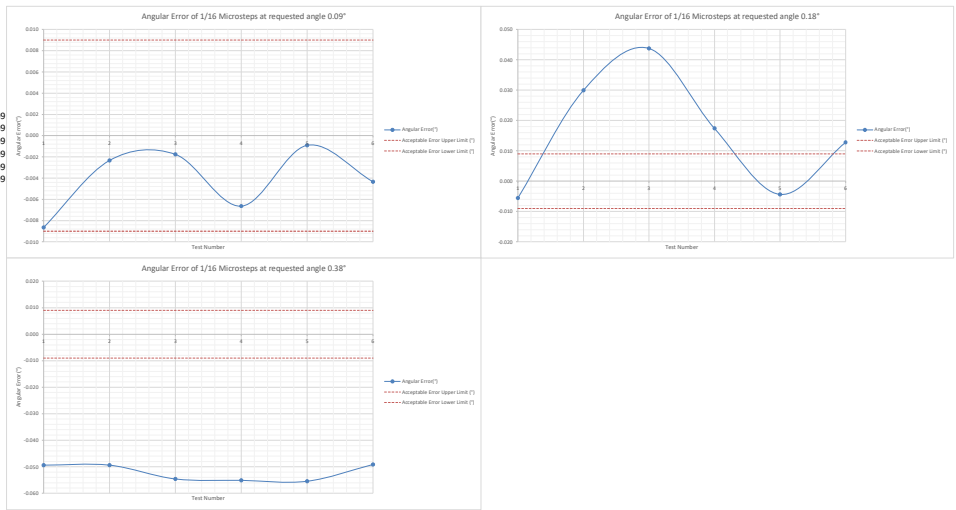


eighth Steps

Test #	Commanded Angle (°)	Actual Angle(°)	Angular Error(°)	Distance to Wall (mm)	Expected Displacement (mm)	Measured Displacement (mm)	Absolute Error (mm)	Error (%)	Notes
1	0.09	0.09	0.001	2000	3.14	2.84	0.30	9.60	16 microstep interp off
2	0.09	0.09	-0.002	2000	3.14	3.06	0.08	2.60	
3	0.09	0.09	-0.002	2000	3.14	3.08	0.08	2.67	
4	0.09	0.088	-0.007	2000	3.14	2.91	0.23	7.37	
5	0.09	0.089	-0.001	2000	3.14	3.11	0.03	1.01	
6	0.09	0.086	-0.004	2000	3.14	2.99	0.15	4.83	
1	0.18	0.174	-0.006	2000	6.28	6.09	0.19	3.07	16 microstep interp off
2	0.18	0.210	0.030	2000	6.28	7.33	1.05	16.66	
3	0.18	0.224	0.044	2000	6.28	7.81	1.53	24.30	
4	0.18	0.197	0.017	2000	6.28	6.89	0.61	9.66	
5	0.18	0.176	-0.004	2000	6.28	6.13	0.15	2.44	
6	0.18	0.151	-0.013	2000	6.28	6.73	0.45	7.11	
1	0.38	0.331	-0.049	2000	13.26	11.54	1.72	13.00	16 microstep interp off
2	0.38	0.321	-0.049	2000	13.26	11.54	1.72	13.00	
3	0.38	0.325	-0.055	2000	13.26	11.36	1.90	14.36	
4	0.38	0.325	-0.055	2000	13.26	11.34	1.92	14.51	
5	0.38	0.325	-0.055	2000	13.26	11.33	1.93	14.59	
6	0.38	0.331	-0.049	2000	13.26	11.55	1.71	12.93	

Average 0.88  
Max 1.93  
Min 0.03  
StDev 0.031210579

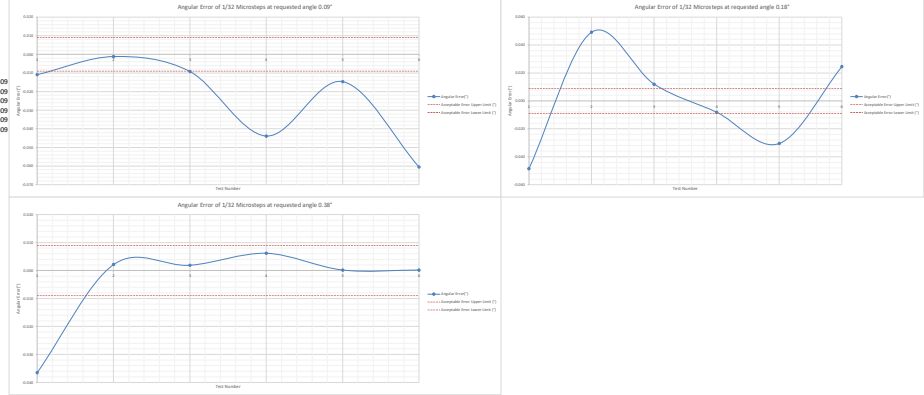
Acceptable Error      Acceptable Error Upper Limit (°)      Acceptable Error Lower Limit (°)  
1 0.009 -0.009  
2 0.009 -0.009  
3 0.009 -0.009  
4 0.009 -0.009  
5 0.009 -0.009  
6 0.009 -0.009



Test #	Commanded Angle (°)	Actual Angle(°)	Angular Error(°)	Distance to Wall (mm)	Expected Displacement (mm)	Measured Displacement (mm)	Absolute Error (mm)	Error (%)	Notes
1	0.09	0.079	0.011	2000	3.14	2.76	0.38	12.15	32 microstep interp off
2	0.09	0.089	0.003	2000	3.14	3.1	0.34	1.32	
3	0.09	0.081	0.009	2000	3.14	2.82	0.32	10.24	
4	0.09	0.084	0.011	2000	3.14	2.61	0.51	16.75	
5	0.09	0.075	0.015	2000	3.14	2.63	0.51	16.28	
6	0.09	0.030	0.060	2000	3.14	1.03	2.11	67.21	
1	0.11	0.111	0.001	2000	4.59	4.59	0.00	0.00	32 microstep interp off
2	0.18	0.229	0.049	2000	6.28	8	1.77	27.32	32 microstep interp off
3	0.18	0.192	0.012	2000	6.28	6.7	0.42	6.63	bending is slightly off
4	0.18	0.177	0.023	2000	6.28	6	0.38	5.98	
5	0.18	0.150	0.030	2000	6.28	5.22	1.06	18.62	
6	0.18	0.205	0.025	2000	6.28	7.14	0.86	11.64	
1	0.31	0.341	0.031	2000	11.59	11.59	0.00	0.00	32 microstep interp off
2	0.38	0.382	0.002	2000	13.26	13.34	0.08	0.57	
3	0.38	0.382	0.002	2000	13.26	13.33	0.07	0.49	
4	0.38	0.346	0.036	2000	13.26	13.45	0.27	1.97	
5	0.38	0.380	0.000	2000	13.26	13.27	0.01	0.04	
6	0.38	0.380	0.000	2000	13.26	13.27	0.01	0.04	

Average 0.70  
Max 2.11  
Min 1.03  
StdDev 0.026932405

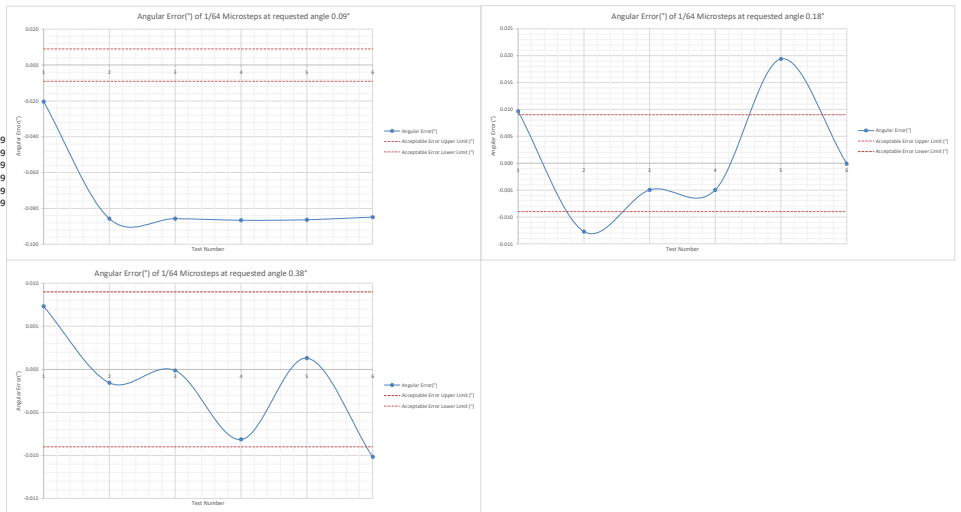
Acceptable Error  
Acceptable Error Upper Limit (°) 0.000  
1 0.009  
2 0.009  
3 0.009  
4 0.009  
5 0.009  
6 0.009



Test #	Commanded Angle (°)	Actual Angle (°)	Angular Error (°)	Distance to Wall (mm)	Expected Displacement (mm)	Measured Displacement (mm)	Absolute Error (mm)	Error (%)	Notes
1	0.09	0.070	-0.020	2000	3.14	2.43	0.712	22.65	64 microstep interp off. Must have been at a point where it could get past static friction.
2	0.09	0.004	-0.086	2000	3.14	0.15	2.992	95.23	Backlash? Not enough Torque to drive Stage at this angle
3	0.09	0.004	-0.086	2000	3.14	0.15	2.992	95.23	Backlash again
4	0.09	0.003	-0.087	2000	3.14	0.12	3.022	96.18	Backlash again
5	0.09	0.004	-0.086	2000	3.14	0.13	3.012	95.86	Backlash again
6	0.09	0.005	-0.085	2000	3.14	0.18	2.962	94.27	Backlash again
1	0.18	0.190	0.010	2000	6.28	6.62	0.337	5.36	64 microstep interp off
2	0.18	0.167	-0.013	2000	6.28	5.94	0.443	7.05	
3	0.18	0.175	-0.005	2000	6.28	6.11	0.134	2.25	
4	0.18	0.175	-0.005	2000	6.28	6.11	0.173	2.76	
5	0.18	0.199	0.019	2000	6.28	6.96	0.677	10.77	
6	0.18	0.180	0.000	2000	6.28	6.28	0.003	0.05	
1	0.38	0.387	0.007	2000	13.26	13.52	0.255	1.92	64 microstep interp off
2	0.38	0.378	-0.002	2000	13.26	13.21	0.055	0.41	
3	0.38	0.380	0.000	2000	13.26	13.26	0.005	0.04	
4	0.38	0.372	-0.008	2000	13.26	12.98	0.285	2.15	
5	0.38	0.381	0.001	2000	13.26	13.31	0.045	0.34	
6	0.38	0.370	-0.010	2000	13.26	12.91	0.355	2.67	

Average 1.03  
 Max 3.02  
 Min 0.00  
 StDev 0.039607204

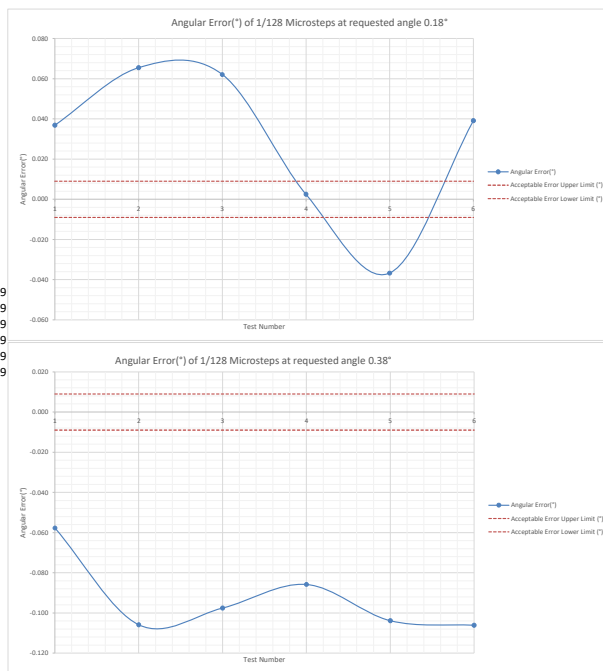
Acceptable Error  
 Acceptable Error Upper Limit (°) 0.009  
 Acceptable Error Lower Limit (°) -0.009  
 1 0.009  
 2 0.009  
 3 0.009  
 4 0.009  
 5 0.009  
 6 0.009



Test #	Commanded Angle (°)	Actual Angle(°)	Angular Error(°)	Distance to Wall (mm)	Expected Displacement (mm)	Measured Displacement (mm)	Absolute Error (mm)	Error (%)	Notes
1	0.18	0.217	0.037	2000	6.28	7.57	1.29	20.5	128 microstep, interp off
2	0.18	0.246	0.066	2000	6.28	8.57	2.29	36.4	
3	0.18	0.242	0.062	2000	6.28	8.45	2.17	34.5	
4	0.18	0.182	0.002	2000	6.28	6.37	0.09	1.4	
5	0.18	0.143	-0.037	2000	6.28	5	1.28	20.4	
6	0.18	0.219	0.039	2000	6.28	7.65	1.37	21.8	
1	0.38	0.322	-0.058	2000	13.26	11.25	2.01	15.2	128 microstep, interp off
2	0.38	0.274	-0.106	2000	13.26	9.57	3.69	27.9	
3	0.38	0.282	-0.098	2000	13.26	9.86	3.40	25.7	
4	0.38	0.294	-0.086	2000	13.26	10.27	2.99	22.6	
5	0.38	0.276	-0.104	2000	13.26	9.64	3.62	27.3	
6	0.38	0.274	-0.106	2000	13.26	9.56	3.70	27.9	

Average 2.33  
 Max 3.70  
 Min 0.09  
 StDev 0.069629954

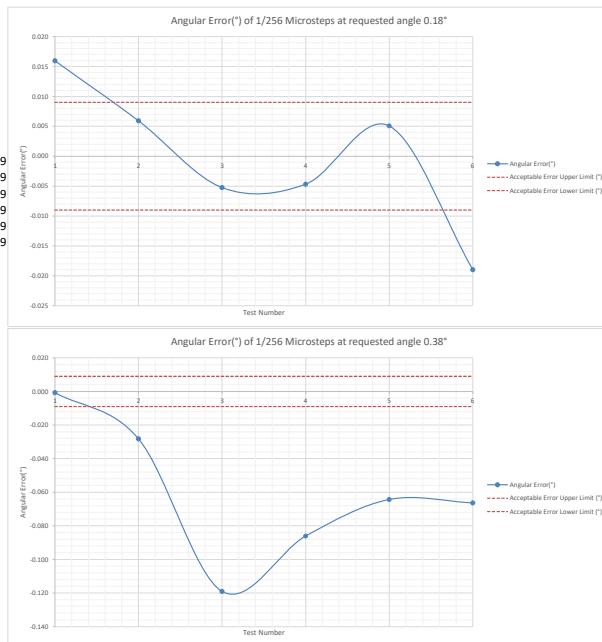
Acceptable Error	Acceptable Error Upper Limit (°)	Acceptable Error Lower Limit (°)
1	0.009	-0.009
2	0.009	-0.009
3	0.009	-0.009
4	0.009	-0.009
5	0.009	-0.009
6	0.009	-0.009



Test #	Commanded Angle (°)	Actual Angle(°)	Angular Error(°)	Distance to Wall (mm)	Expected Displacement (mm)	Measured Displacement (mm)	Absolute Error (mm)	Error (%)	Notes
1	0.18	0.196	0.016	2000	6.28	6.84	0.557	8.9	256 microstep, interp off
2	0.18	0.186	0.006	2000	6.28	6.49	0.207	3.3	256 microstep, interp off
3	0.18	0.175	-0.005	2000	6.28	6.1	0.183	2.9	256 microstep, interp off
4	0.18	0.175	-0.005	2000	6.28	6.12	0.163	2.6	256 microstep, interp off
5	0.18	0.185	0.005	2000	6.28	6.46	0.177	2.8	256 microstep, interp off
6	0.18	0.161	-0.019	2000	6.28	5.62	0.663	10.6	256 microstep, interp off
1	0.38	0.379	-0.001	2000	13.26	13.24	0.025	0.2	256 microstep, interp off
2	0.38	0.352	-0.028	2000	13.26	12.28	0.985	7.4	256 microstep, interp off
3	0.38	0.261	-0.119	2000	13.26	9.11	4.155	31.3	256 microstep, interp off
4	0.38	0.294	-0.086	2000	13.26	10.26	3.005	22.7	256 microstep, interp off
5	0.38	0.316	-0.064	2000	13.26	11.02	2.245	16.9	256 microstep, interp off
6	0.38	0.314	-0.066	2000	13.26	10.95	2.315	17.5	256 microstep, interp off

Average 1.22  
 Max 4.15  
 Min 0.02  
 StDev 0.043094114

Acceptable Error	Acceptable Error Upper Limit (°)	Acceptable Error Lower Limit (°)
1	0.009	-0.009
2	0.009	-0.009
3	0.009	-0.009
4	0.009	-0.009
5	0.009	-0.009
6	0.009	-0.009



## 8.4 Gantt Chart

Plan owner	Gabriel Pierce										
Project start date	20/03/2025										
Project finish date	04/07/2025										
Duration	80 days										
% complete	5%										
Exported on	02/07/2025										
Task number	Outline number	Name	Assigned to	Start	Finish	Duration	Bucket	% complete	Depends on	Dependents (after)	
1	1	Literature review and Requirements definition		17/03/2025	08/04/2025	17 days	Bucket 1	0%			
2	1.1	Initial Research		17/03/2025	17/03/2025	1 day	Bucket 1	0%		3FS	
3	1.2	Optical Applications research Write up		18/03/2025	20/03/2025	3 days	Bucket 1	0%	2FS	4FS	
4	1.3	CAL Writeup		21/03/2025	25/03/2025	3 days	Bucket 1	0%	3FS	5FS	
5	1.4	Closed loop Motor Research Write up		26/03/2025	27/03/2025	2 days	Bucket 1	0%	4FS	6FS	
6	1.5	Material Selection Write Up		28/03/2025	31/03/2025	2 days	Bucket 1	0%	5FS	7FS	
7	1.6	Bearing Research Write up		01/04/2025	02/04/2025	2 days	Bucket 1	0%	6FS	8FS, 27FS	
8	1.7	Cycloidal Drive design Research Write Up		03/04/2025	04/04/2025	2 days	Bucket 1	0%	7FS	9FS, 11FS, 27FS	
9	1.8	Software/firmware/ control algorithm research		07/04/2025	08/04/2025	2 days	Bucket 1	0%	8FS		
10	2	Mechanical Design		20/03/2025	11/04/2025	17 days	Bucket 1	0%			
11	2.1	Cycloidal Drive Parameter Selection		07/04/2025	07/04/2025	1 day	Bucket 1	0%	8FS	12FS, 14FS, 27FS	
12	2.2	Cycloidal Disk Sketch / Mockup		08/04/2025	08/04/2025	1 day	Bucket 1	0%	11FS	13FS, 16FS, 27FS	
13	2.3	Motor Housing Sketch/ Mockup		09/04/2025	09/04/2025	1 day	Bucket 1	0%	12FS	15FS	
14	2.4	Bearing's Sketch/Mockup		08/04/2025	08/04/2025	1 day	Bucket 1	0%	11FS	27FS	
15	2.5	Motor Mount Sketch/Mockup		10/04/2025	10/04/2025	1 day	Bucket 1	0%	13FS	17FS	
16	2.6	Motor Output Design		09/04/2025	09/04/2025	1 day	Bucket 1	0%	12FS		
17	2.7	4040 Rail Mount		11/04/2025	11/04/2025	1 day	Bucket 1	0%	15FS		
18	2.8	First Draft Complete		20/03/2025	20/03/2025	1 day	Bucket 1	0%		27FS	
19	3	Electronics & PCB7 Design		10/04/2025	17/04/2025	6 days	Bucket 1	0%		33FS	
20	3.1	Electrical Component Selection		10/04/2025	10/04/2025	1 day	Bucket 1	0%		21FS, 33FS	
21	3.2	Circuit design		11/04/2025	11/04/2025	1 day	Bucket 1	0%	20FS	22FS	
22	3.3	Verify circuit works through sim + prototype		14/04/2025	14/04/2025	1 day	Bucket 1	0%	21FS	23FS	
23	3.4	Breadboard testing		15/04/2025	15/04/2025	1 day	Bucket 1	0%	22FS	24FS	
24	3.5	Initial PCB design		16/04/2025	16/04/2025	1 day	Bucket 1	0%	23FS	25FS	
25	3.6	Send files to PCBway		17/04/2025	17/04/2025	1 day	Bucket 1	0%	24FS		
26	4	Finalise design and Order Components		09/04/2025	15/04/2025	5 days	Bucket 1	40%			
27	4.1	Component Selection		09/04/2025	09/04/2025	1 day	Bucket 1	0%	8FS, 11FS, 12FS, 28FS		
28	4.2	Finalise SOLIDWORKS Parts		10/04/2025	10/04/2025	1 day	Bucket 1	0%	27FS	29FS, 30FS	
29	4.3	Finalise SOLIDWORKS Assembly		11/04/2025	11/04/2025	1 day	Bucket 1	0%	28FS	30FS	
30	4.4	First Test prints		14/04/2025	14/04/2025	1 day	Bucket 1	100%	29FS, 28FS	31FS	
31	4.5	Print & Assemble First prototype		15/04/2025	15/04/2025	1 day	Bucket 1	100%	30FS	37FS	
32	5	Firmware Development/ Coding & Motion Te		18/04/2025	23/04/2025	4 days	Bucket 1	0%			
33	5.1	Install firmware on Raspberry pi		18/04/2025	18/04/2025	1 day	Bucket 1	0%	20FS, 19FS	34FS, 36FS, 37FS	
34	5.2	Create Configuration for Firmware		21/04/2025	21/04/2025	1 day	Bucket 1	0%	33FS	36FS, 37FS, 35FS	
35	5.3	Testing code		22/04/2025	22/04/2025	1 day	Bucket 1	0%	34FS	37FS	
36	5.4	Full system Assembly & Debugging		23/04/2025	23/04/2025	1 day	Bucket 1	0%		33FS, 34FS	
37	5.4.1	Accuracy & Vibration Testing		23/04/2025	23/04/2025	1 day	Bucket 1	0%		31FS, 34FS, 33F	
38	5.4.2	Implementing & tuning Input Shaping					Bucket 1	0%			
39	5.4.3	Performance & Results Analysis					Bucket 1	0%			
40	6	Final Refinements		04/07/2025	04/07/2025	1 day	Bucket 1	0%			
41	6.1	Write Technical Report & EDI Consideration					Bucket 1	0%			
42	6.2	Create A3 Poster					Bucket 1	0%			
43	6.3	Final Testing & submission		04/07/2025	04/07/2025	1 day	Bucket 1	0%			

Figure 8.2: Initial rough project plan

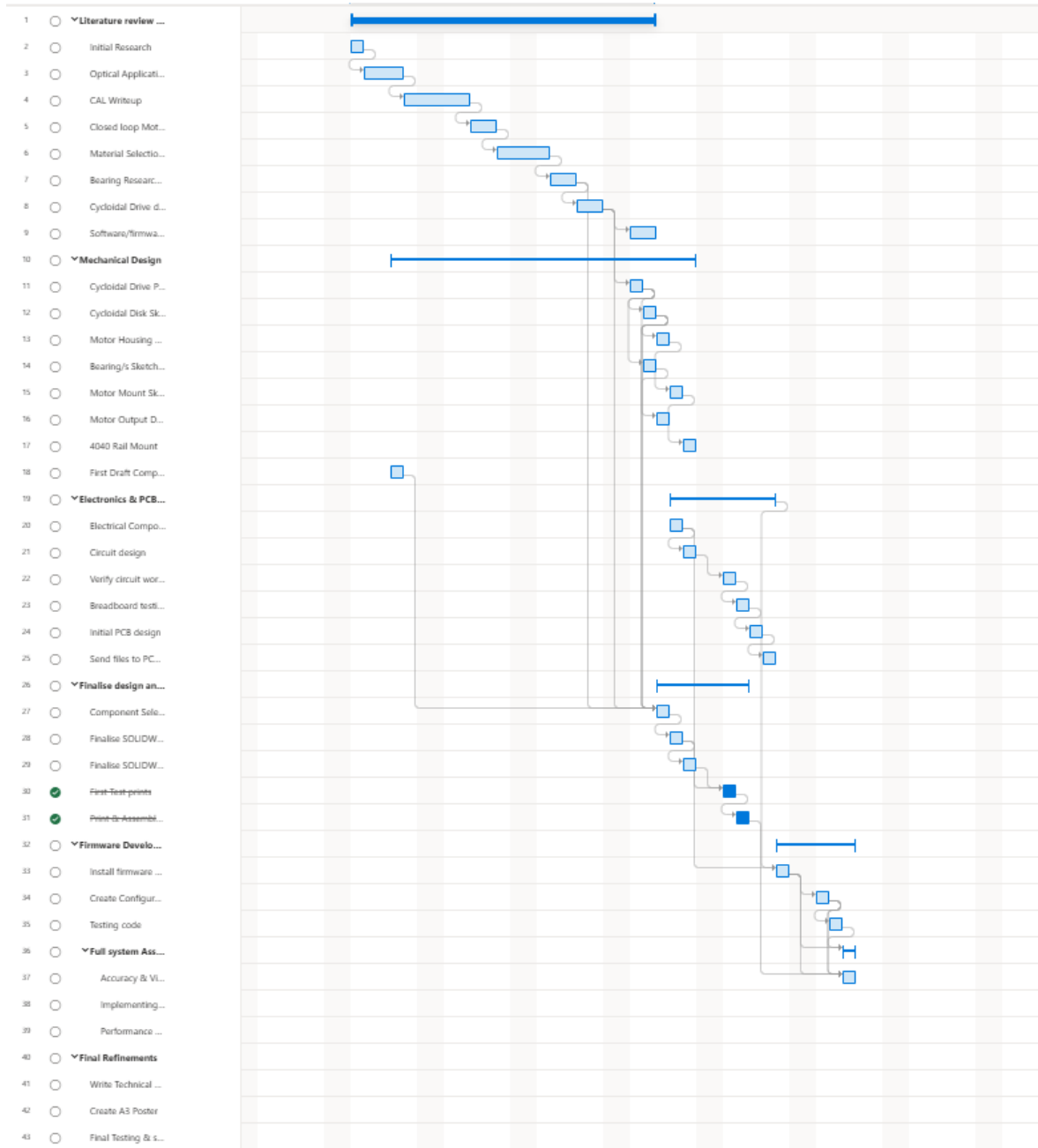


Figure 8.3: Gantt chart